A Lagrangian Model for Baroclinic Genesis of Mesoscale Vortices. Part I: Theory

ROBERT DAVIES-JONES

NOAA/National Severe Storms Laboratory, Norman, Oklahoma

(Manuscript received 14 August 1998, in final form 5 May 1999)

ABSTRACT

The problem of weakly stratified, weakly sheared flow over (or under) obstacles is solved approximately by using a Lagrangian approach that obtains solutions on isentropic or Bernoulli surfaces and hence reveals the vortex lines immediately. The new method is based on a decomposition of the vorticity in dry, inviscid, isentropic flow into baroclinic and barotropic components. The formulas for both baroclinic and barotropic vorticity are exact formal solutions of the vorticity equation. A nonhydrostatic Lagrangian model approximates these solutions based on a primary-flow–secondary-flow approach. The assumed primary flow is a three-dimensional steady potential flow so that it is a solution of the governing inviscid equations only in the absence of stratification and preexisting vorticity. It is chosen to be irrotational in order to eliminate the primary flow as the origin of rotation. Three particular potential flows are chosen for their simplicity and because pieces of them approximate mesoscale atmospheric flows. The secondary flow is the correction needed to give an improved approximation to the actual flow. The Lagrangian model computes the secondary vorticity that develops owing to the introduction of stratification and vorticity in the upstream horizontally homogeneous environment as secondary effects without modification of the primary flow. Potential vorticity is conserved and is zero because both the barotropic and the baroclinic vortex lines lie in the isentropic surfaces.

The baroclinic component of vorticity, zero initially, depends on the gradient of cumulative temperature (the Lagrangian integral of temperature following an air parcel) and on the local entropy gradient. In a particular isentropic surface, it is determined by the local static stability and by horizontal gradients of the height and the cumulative height perturbations of parcels in the surface. For weak stable stratification, it is proven that the vertical baroclinic vorticity is cyclonic (anticyclonic) on the entire right (left) side of the flow, upstream as well as downstream of the height extremum. A time-dependent linearized version of the model is used to show how the baroclinic vortex lines evolve initially.

Barotropic vorticity is determined by the property that barotropic vortex lines, which are straight and horizontal in the upstream environment, are frozen into the fluid and move with it. The component normal to the surfaces of the secondary velocity induced by the baroclinic and barotropic vorticity is deduced qualitatively.

1. Introduction

Baroclinic generation of vorticity plays a role in numerous atmospheric flows including tornadic storms (Klemp and Rotunno 1983; Rotunno and Klemp 1985; Davies-Jones and Brooks 1993); stably stratified flow over and around obstacles (Hawthorne and Martin 1955; Scorer 1978), hills (Smolarkiewicz and Rotunno 1989), and penetrating cloud tops; mesoscale convective systems (Weisman 1993; Weisman and Davis 1998); mesoscale convective vortices (Brandes 1990); and even large-scale flows where, in thermal-wind balance, it counterbalances tilting of the earth's vorticity toward the horizontal by vertical wind shear (Davies-Jones 1991). A Lagrangian model of the generation of baroclinic vortices in inviscid, isentropic flows in horizontally homogeneous environments is developed here. Because the earth's rotation is neglected, the study is limited to small scales and to the first three or four hours in the lives of various systems. This paper is the first of two articles. In this paper (Part I), the theory of the Lagrangian model is developed. In Part II, model results for dry, stably stratified flow over obstacles at high internal Froude number will be presented to demonstrate that the model correctly predicts the baroclinic genesis of vortices in the lee of hills and of penetrating cloud tops. The theory then will be adapted to apply approximately to moist convection in conditionally unstable stratification, and the model will be used to show how rear-inflow jets and bookend vortices might form in mesoscale convective systems and how the low-level parent circulation of tornadoes might develop in supercell and bow-echo storms.

Essentially this paper revamps the investigations of Hawthorne and Martin (1955) and Drazin (1961) of stratified sheared flow over (or under) obstacles by using a Lagrangian approach that obtains solutions on isen-

Corresponding author address: Dr. Robert Davies-Jones, National Severe Storms Laboratory, NOAA, 1313 Halley Circle, Norman, OK 73069-8493.
E-mail: bobdj@nssl.noaa.gov

tropic or Bernoulli surfaces and hence reveals the vortex lines immediately. The model also may be considered to be an improvement of Smolarkiewicz and Rotunno's (1989) linear theory, which correctly explained the development of vertical vorticity in the lee but was unable to provide an estimate of the magnitude of the vorticity. The new method is based on a decomposition of the vorticity in dry, inviscid, isentropic flow into baroclinic and barotropic components as formulated by Dutton (1976) and Mobbs (1981). The formulas for baroclinic and barotropic vorticity are exact formal solutions of the vorticity equation. The Lagrangian model approximates these solutions based on a primary flow–secondary flow approach (Drazin 1961; Taylor 1972). This contrasts with customary theories in meteorology (e.g., quasi- and semigeostrophic theories) that seek solutions of adulterated versions of the vector vorticity equation. The assumed primary flow is a three-dimensional steady potential flow so that it is a solution of the governing inviscid equations only in the absence of stratification and preexisting vorticity. It is a rudimentary description of the actual flow. The primary flow is chosen to be irrotational in order to eliminate the primary flow as the origin of rotation. Effects of buoyancy on the primary flow are omitted out of necessity, even though strong stratification reduces markedly the decay of a disturbance with height (Smith 1979). The particular potential flows used in this paper are chosen for their simplicity and because pieces of them approximate mesoscale atmospheric flows. A previous version of the model (Davies-Jones 1996) suffered from unrealistic or undesirable features such as a uniform horizontal wind, no variation of vertical velocity with height, and a minor amount of vorticity in the primary flow owing to horizontal gradients of vertical velocity. The secondary flow is the correction needed to give an improved approximation to the actual flow. The Lagrangian model computes the secondary vorticity that develops owing to the introduction of stratification and vorticity in the upstream horizontally homogeneous environment as secondary effects without modification of the primary flow. The isentropic surfaces, which are material surfaces that are horizontal upstream, are deformed by the potential flow, giving rise to horizontal temperature gradients. The deformation of the isentropic surfaces may be a result of air flowing over a hill or of vertical displacements associated with convective updrafts and downdrafts. Potential vorticity is conserved and is zero because both the barotropic and the baroclinic vortex lines lie in the isentropic surfaces. According to Dutton's formula, the baroclinic component of vorticity depends on the gradient of cumulative temperature and on the local entropy gradient. Cumulative temperature is defined as the Lagrangian integral of temperature, that is, the integral over time of temperature following an air parcel. Barotropic vorticity is determined by the property that barotropic vortex lines, which are straight and horizontal in the upstream environment, are frozen into the fluid and move with it. Significant vertical vorticity develops in the model from baroclinic effects even in the complete absence of upstream vorticity.

The model is nonhydrostatic. It is also nonlinear in some respects; for example, it is not limited to quasi-horizontal motions. But it is linear in the respect that the secondary vorticity acts like a passive vector because it is determined by the irrotational primary flow, which is decoupled from it. Associated with the secondary vorticity is a secondary velocity, which can be computed. Thus a nonlinear tertiary vorticity could be obtained in principle. However, the mathematics is intractable at this stage. Scorer (1978) devotes an entire chapter of his book to the topic of secondary streamwise vorticity, which he simply calls secondary vorticity. A time-dependent linear version of the model is used to show how the baroclinic vortex lines evolve initially.

The Lagrangian model was developed to isolate the essential vorticity dynamics of baroclinic vortices, with special emphasis on the vertical vorticity component [in contrast to Hawthorne and Martin (1955), Drazin (1961) and Scorer (1978), who demonstrated the formation of streamwise vorticity (component along the streamlines) and to Eames and Hunt (1997), who calculated the forces acting on a body moving in a weak density gradient]. Complex numerical models naturally are more realistic, but dynamical explanations of how vortices form within them are still based on relatively simple conceptual models that fit numerical results and diagnostic computations.

2. Barotropic and baroclinic vorticity

Dutton (1976, 387–390) showed from an integral of the vector vorticity equation that absolute vorticity $\boldsymbol{\omega}$ in dry, inviscid, isentropic flows is the sum of barotropic and baroclinic components, $\boldsymbol{\omega}_{\mathrm{BT}}$ and $\boldsymbol{\omega}_{\mathrm{BC}}$, respectively. This decomposition is dependent on the arbitrary choice of the initial time, $t = 0$. The barotropic vorticity at a subsequent (or ''current'') time t is the vorticity that develops from the amplification and reorientation of initial relative vorticity and the earth's vorticity in the absence of baroclinic generation. Barotropic vortex lines are ''frozen'' into the fluid and behave like elastic strings that the flow moves, stretches, and reorients. Thus, the current barotropic vorticity of a parcel depends on initial vorticity and on the initial and current positions of the parcel and its neighbors along the vortex line through the parcel, but is independent of the paths taken by the parcels to get from their initial to their current positions. On the other hand, baroclinic vorticity consists of vorticity that has been generated as quasi-horizontal vorticity by the baroclinic term since $t = 0$ and has been subsequently affected by vortex-tube stretching and tilting. The baroclinic vorticity of a parcel depends on its cumulative or accumulated temperature since $t = 0$. The baroclinic vortex lines lie in isentropic surfaces; hence the baroclinic component does not contribute to poten-

tial vorticity. In a stratified horizontally homogeneous environment, baroclinic vorticity is associated with the temperature gradients caused by the vertical displacements of parcels and isentropic surfaces. Dutton's statement that the isentropic surfaces and baroclinic vorticity are primarily horizontal in the atmosphere applies to flows with low height to length ratios but not to tornadoes.

3. Vorticity decomposition for dry isentropic flows

From differentiation of Poisson's equation for θ,

$$-\alpha\nabla p = T\nabla S - \nabla(c_p T), \tag{3.1}$$

where $\alpha \equiv 1/\rho$, ρ, p, T; $S \equiv c_p \ln(\theta/\theta_0)$; $c_p T$ are the specific volume, density, pressure, temperature, specific entropy, and specific enthalpy, respectively, of dry air; c_p is the specific heat of dry air at constant pressure; θ is potential temperature; and θ_0 is a reference value of θ. Hence, the sum of the accelerations due to gravity, $-g_a\mathbf{k}$, and the pressure-gradient force may be expressed by

$$-\alpha\nabla p - g_a\mathbf{k} \equiv T\nabla S - \nabla(c_p T + g_a z). \tag{3.2}$$

Thus, the inviscid equations of motion become

$$\frac{d_a\mathbf{u}}{dt} \equiv \frac{\partial\mathbf{v}}{\partial t} + (\mathbf{v}\cdot\nabla)\mathbf{v} + 2\boldsymbol{\Omega}\times\mathbf{v} - \nabla(|\boldsymbol{\Omega}\times\mathbf{r}|^2/2)$$
$$= -\nabla(c_p T + g_a z) + T\nabla S \tag{3.3a}$$

or, equivalently,

$$\frac{\partial\mathbf{v}}{\partial t} - \mathbf{v}\times\boldsymbol{\omega} = -\nabla B + T\nabla S, \tag{3.3b}$$

where $\mathbf{v}$ is the wind vector $\equiv (u, v, w)$ in the customary Cartesian coordinates (x, y, z), $\boldsymbol{\omega} \equiv \nabla\times\mathbf{v} + 2\boldsymbol{\Omega}$ is the absolute vorticity vector, $\boldsymbol{\Omega}$ is the earth's angular velocity, $\mathbf{u} \equiv \mathbf{v} + \boldsymbol{\Omega}\times\mathbf{r}$ is the absolute velocity, d_a/dt is the absolute material derivative, $\mathbf{r}$ is the position vector from the earth's center, $\sigma \equiv c_p T + g_a z - |\boldsymbol{\Omega}\times\mathbf{r}|^2/2$ is the static energy, and the sum of static and kinetic energies $B \equiv \sigma + \mathbf{v}\cdot\mathbf{v}/2$ is the Bernoulli function. The centrifugal potential $-|\boldsymbol{\Omega}\times\mathbf{r}|^2/2$ and gravitational potential $g_a z$ can be combined with negligible error into an effective-gravity potential gz (Haltiner and Martin 1957, p. 161). Hence $\sigma \equiv c_p T + gz$. When the flow is steady and barotropic, the surfaces of constant B are called Bernoulli or Lamb surfaces. These are normal to $\mathbf{v}\times\boldsymbol{\omega}$ and thus are crisscrossed by a network of streamlines and vortex lines. The continuity equation is

$$d\ln\alpha/dt = \nabla\cdot\mathbf{v}, \tag{3.4}$$

and the thermodynamic energy equation for isentropic flow is simply

$$dS/dt = 0. \tag{3.5}$$

From the ideal gas law and the definitions of S and θ,

$$R\ln\alpha = S - c_v\ln T + c_p\ln\theta_0 + R\ln(R/p_0), \tag{3.6}$$

where R is the gas constant for dry air, $c_v \equiv c_p - R$ is the specific heat of dry air at constant volume, and $p_0 \equiv 1000$ mb. Equations (3.3)–(3.6) are a closed system of equations in the six variables u, v, w, T, α, S.

Taking the curl of (3.3) and using (3.4) yields the vector vorticity equation

$$\frac{d}{dt}(\alpha\boldsymbol{\omega}) = (\alpha\boldsymbol{\omega}\cdot\nabla)\mathbf{v} + \alpha\nabla T\times\nabla S, \tag{3.7a}$$

or, equivalently,

$$\frac{\partial\boldsymbol{\omega}}{\partial t} - \nabla\times(\mathbf{v}\times\boldsymbol{\omega}) = \nabla T\times\nabla S, \tag{3.7b}$$

where $\nabla T\times\nabla S \equiv -\nabla\alpha\times\nabla p$ is the baroclinic-generation or solenoidal term, or solenoid or baroclinity vector. The desired vorticity decomposition is

$$\boldsymbol{\omega}(x, y, z, t) = \boldsymbol{\omega}_{\mathrm{BT}}(x, y, z, t) + \boldsymbol{\omega}_{\mathrm{BC}}(x, y, z, t), \tag{3.8}$$

where $\boldsymbol{\omega}_{\mathrm{BC}}$ is a solution of (3.7); $\boldsymbol{\omega}_{\mathrm{BT}}$ is a solution of the barotropic version of (3.7), which is the necessary and sufficient condition for frozen $\boldsymbol{\omega}_{\mathrm{BT}}$ lines (Borisenkov and Tarapov 1979, p. 240); and the components satisfy the initial conditions

$$\boldsymbol{\omega}_{\mathrm{BT}}(x, y, z, 0) = \boldsymbol{\omega}(x, y, z, 0),$$
$$\boldsymbol{\omega}_{\mathrm{BC}}(x, y, z, 0) = 0. \tag{3.9}$$

The formula for barotropic vorticity, first derived by A.-L. Cauchy in 1815, is (in Cartesian–tensor notation)

$$(\alpha\boldsymbol{\omega}_{\mathrm{BT}})_j(x_1, x_2, x_3, t) = \frac{\partial x_j}{\partial X_i}(\alpha\boldsymbol{\omega}_{\mathrm{BT}})_i(X_1, X_2, X_3, 0), \tag{3.10}$$

where $\mathbf{X} \equiv (X_1, X_2, X_3) \equiv (X, Y, Z)$ are the initial coordinates of a parcel currently at $\mathbf{x} \equiv (x_1, x_2, x_3) \equiv (x, y, z)$. See appendix A for proof that (3.10) is a solution of the barotropic version of (3.7a).

The formula for baroclinic vorticity was discovered by Dutton (1976) and Mobbs (1981). It is

$$\boldsymbol{\omega}_{\mathrm{BC}} = \nabla\Lambda\times\nabla S, \tag{3.11}$$

where $\Lambda \equiv \int_0^t T\, d\hat{t}_P$ is the cumulative temperature, the appended subscript P denotes that the integral is a Lagrangian one (following a parcel), and $\hat{}$ signifies a dummy variable of integration. Dutton's direct proof involved derivation of the following implicit formula for velocity in inviscid, isentropic flow (see also Serrin 1959; Mobbs 1981):

$$\mathbf{u} = \Lambda\nabla S - \nabla\Phi + \nabla\mathbf{X}\cdot\mathbf{u}_0, \tag{3.12}$$

where $d\Phi/dt \equiv c_p T + g_a z - \mathbf{u}\cdot\mathbf{u}/2$, $-\nabla\Phi = \nabla\int_0^t (\mathbf{u}\cdot\mathbf{u}/2 - c_p T - g_a z)\, d\hat{t}_P$ is the gradient of the cumulative difference between absolute kinetic and static energies, $\mathbf{u}_0$ is the initial absolute velocity, and $\nabla\mathbf{X}\cdot\mathbf{u}_0 \equiv (\partial X_k/\partial x_j)(u_0)_k$. An easier indirect proof involves substitution of (3.11) into (3.7b) and use of some vector identities to verify that (3.11) is indeed a solution of the vorticity equation when S is conserved (see appendix

A). A similar proof (appendix A) verifies (3.12) by showing that its material derivative satisfies (3.3a) when (3.5) holds. Note that the curl of the first term on the right of (3.12) gives the baroclinic vorticity; the second term is irrotational; and as proven generally by Dutton (1976, 388–389) and in sections 12–13 for shear flows in horizontally homogeneous environments, the curl of the third term yields the barotropic vorticity. This decomposition of velocity into rotational and potential components is not unique because of the identity $\Lambda\boldsymbol{\nabla}S = \boldsymbol{\nabla}(\Lambda S) - S\boldsymbol{\nabla}\Lambda$. Clearly, the rotational component can contain a large irrotational part that can cancel a large part of the potential component. Hence, the total velocity can be small compared to the individual components. Note that Weber's transformed equations of motion (Serrin 1959) under the constraints of mass continuity and entropy conservation yield the velocity formula (3.12) and the definitions $d\Lambda/dt = T$ and $d\Phi/dt = c_pT + g_az - \mathbf{u}\cdot\mathbf{u}/2$ (Serrin 1959; Dutton 1976; Mobbs 1981; Salmon 1988).

We actually use a slightly different version of (3.11),

$$\boldsymbol{\omega}_{\mathrm{BC}} = \boldsymbol{\nabla}_S\Lambda \times \boldsymbol{\nabla}S, \tag{3.13}$$

obtained by recalling that the gradient of Λ in height coordinates is related to the gradient of Λ on an isentropic surface by

$$\begin{aligned}\boldsymbol{\nabla}\Lambda(x, y, z, t) &= \boldsymbol{\nabla}\Lambda(x, y, S(x, y, z), t)\\ &= \boldsymbol{\nabla}_S\Lambda + \frac{\partial\Lambda}{\partial S}\boldsymbol{\nabla}S,\end{aligned} \tag{3.14}$$

where $\boldsymbol{\nabla}_s\Lambda \equiv ((\partial\Lambda/\partial x)_S, (\partial\Lambda/\partial y)_S, 0)$ (Dutton 1976, p. 244). By integrating (3.11) over a material surface $A(t)$ that is bounded by the closed material curve $C(t)$ and applying Stokes's theorem, we find that the baroclinic circulation $\Gamma_{\mathrm{BC}}(t)$ around $C(t)$ is given by

$$\begin{aligned}\Gamma_{\mathrm{BC}}(t) &= \iint_{A(t)} \boldsymbol{\omega}_{\mathrm{BC}}\cdot d\mathbf{A} = \iint_{A(t)} (\boldsymbol{\nabla}\Lambda \times \boldsymbol{\nabla}S)\cdot d\mathbf{A}\\ &= \oint_{C(t)} \Lambda\boldsymbol{\nabla}S\cdot d\mathbf{x},\end{aligned} \tag{3.15}$$

where $\Gamma_{\mathrm{BC}}(0) \equiv 0$ because $\Lambda \equiv 0$ at the initial time. The absolute barotropic circulation around $C(t)$ is conserved; that is,

$$(\Gamma_a)_{\mathrm{BT}}(t) \equiv \oint_{C(t)} \mathbf{u}\cdot d\mathbf{x} - \Gamma_{\mathrm{BC}}(\mathbf{t}) = (\Gamma_a)_{\mathrm{BT}}(0). \tag{3.16}$$

The absolute circulation $\Gamma_a(t)$ around $C(t)$ is the sum of the invariant barotropic circulation and the baroclinic circulation (which grows from zero at $t = 0$); that is,

$$\Gamma_a(t) = (\Gamma_a)_{\mathrm{BT}}(0) + \oint_{C(t)} \Lambda\boldsymbol{\nabla}S\cdot d\mathbf{x}. \tag{3.17}$$

Upon reading Dutton's (1976, 364–374) review of circulation theorems, it becomes evident that (3.17) is an integral of Eckart's (1960) circulation theorem

$$\begin{aligned}\frac{d}{dt}\left(\Gamma_a - \oint_{C(t)} \Lambda\boldsymbol{\nabla}S\cdot d\mathbf{x}\right)\\ = -\oint_{C(t)} \Lambda\boldsymbol{\nabla}\frac{dS}{dt}\cdot d\mathbf{x} + \oint_{C(t)} \mathbf{F}\cdot d\mathbf{x}\end{aligned} \tag{3.18}$$

for isentropic ($dS/dt \equiv 0$), frictionless ($\mathbf{F} \equiv 0$) flow. Note that one could reverse the steps and derive (3.11) from the inviscid, isentropic version of (3.18).

Conservation of Ertel's potential vorticity (PV) is easily demonstrated. We repeat Dutton's (1976) proof for later reference. For any scalar Θ, it can be proved, using Cartesian-tensor notation, that

$$\alpha\boldsymbol{\omega}\cdot\frac{d}{dt}\boldsymbol{\nabla}\Theta = \alpha\boldsymbol{\omega}\cdot\boldsymbol{\nabla}\frac{d\Theta}{dt} - \boldsymbol{\nabla}\Theta\cdot[(\alpha\boldsymbol{\omega}\cdot\boldsymbol{\nabla})\mathbf{v}]. \tag{3.19}$$

Thus, taking $\boldsymbol{\nabla}\Theta\cdot$ of (3.7a) yields

$$\frac{d}{dt}(\alpha\boldsymbol{\omega}\cdot\boldsymbol{\nabla}\Theta) = \alpha\boldsymbol{\omega}\cdot\boldsymbol{\nabla}\frac{d\Theta}{dt} + \alpha\boldsymbol{\nabla}\Theta\cdot(\boldsymbol{\nabla}T\times\boldsymbol{\nabla}S). \tag{3.20}$$

If Θ is a conserved quantity and if it is a function only of S and T (or of any other pair of state variables such as α and p), then $d\Theta/dt = 0$ and

$$\begin{aligned}\Theta = \Theta(T, S) &\Rightarrow \boldsymbol{\nabla}\Theta = (\partial\Theta/\partial T)\boldsymbol{\nabla}T + (\partial\Theta/\partial S)\boldsymbol{\nabla}S\\ &\Rightarrow \boldsymbol{\nabla}\Theta\cdot(\boldsymbol{\nabla}T\times\boldsymbol{\nabla}S) = 0,\end{aligned} \tag{3.21}$$

and so (3.20) reduces to

$$\frac{d}{dt}(\alpha\boldsymbol{\omega}\cdot\boldsymbol{\nabla}\Theta) = 0. \tag{3.22}$$

Choosing $\Theta = S$ gives

$$\frac{dQ}{dt} = 0, \tag{3.23}$$

where Ertel's potential vorticity Q is defined here by $Q \equiv \alpha\boldsymbol{\omega}\cdot\boldsymbol{\nabla}S$. Note that $\boldsymbol{\omega}_{\mathrm{BC}}\cdot\boldsymbol{\nabla}S = 0$. Thus, the baroclinic vortex lines lie along the intersections of isentropic surfaces with surfaces of constant Λ. Right-handedness of the trihedral, $\boldsymbol{\nabla}\Lambda$, $\boldsymbol{\nabla}S$, $\boldsymbol{\omega}_{\mathrm{BC}}$, determines the sense of the vorticity.

4. Steady-state relationships for dry isentropic flows

Several other relationships apply if the flow is steady and isentropic (Kanehisa 1996). Then (3.3b)–(3.5) and (3.23) reduce to

$$\boldsymbol{\nabla}B = \mathbf{v}\times\boldsymbol{\omega} + T\boldsymbol{\nabla}S, \tag{4.1}$$

$$\boldsymbol{\nabla}\cdot(\rho\mathbf{v}) = 0, \tag{4.2}$$

$$\mathbf{v}\cdot\boldsymbol{\nabla}S = 0, \tag{4.3}$$

$$\mathbf{v}\cdot\boldsymbol{\nabla}Q = 0, \tag{4.4}$$

where (4.1) is Crocco's theorem (Batchelor 1967, p. 160). The scalar product of (4.1) with $\mathbf{v}$ and (4.3) implies that

$$\mathbf{v} \cdot \nabla B = 0. \tag{4.5}$$

Because the wind vectors lie in the isentropic surfaces (4.3) and the vector $\rho\mathbf{v}$ is solenoidal (4.2), a streamfunction ψ can be defined by

$$\rho\mathbf{v} = \nabla S \times \nabla\psi. \tag{4.6}$$

The streamlines are the intersections of the isentropic surfaces with the stream surfaces ψ = constant. Substituting (4.6) into (4.5) yields

$$\nabla S \times \nabla\psi \cdot \nabla B = 0, \tag{4.7}$$

which implies that $B = B(\psi, S)$; that is, B is constant along a streamline (Haltiner and Martin 1957, p. 177), since the Jacobian of S, ψ, and B (left side) vanishes (Hildebrand 1962, p. 345). Similarly, $Q = Q(\psi, S)$ from (4.6) and (4.4). By taking the vector product of (4.1) with ∇S and using a vector identity, (4.3), (4.6), and the definition of Q, we find that

$$\begin{aligned}\mathbf{J} \equiv \nabla S \times \nabla B &= \nabla S \times (\mathbf{v} \times \boldsymbol{\omega}) \\ &= (\nabla S \cdot \boldsymbol{\omega})\mathbf{v} - (\nabla S \cdot \mathbf{v})\boldsymbol{\omega} = Q\rho\mathbf{v} \\ &= Q\nabla S \times \nabla\psi,\end{aligned} \tag{4.8}$$

where $\mathbf{J}$ is the total flux of potential vorticity (Haynes and McIntyre 1987; Schär 1993). By the chain rule,

$$\nabla B(\psi, S) = \frac{\partial B}{\partial \psi}\nabla\psi + \frac{\partial B}{\partial S}\nabla S. \tag{4.9}$$

Substituting (4.9) into (4.8) yields the relationship

$$Q = \frac{\partial B}{\partial \psi}, \tag{4.10}$$

derived previously by Kanehisa (1996) using tensor instead of vector notation. For a steady isentropic flow with zero potential vorticity, B is a function of S alone so that the isentropic surfaces are also Bernoulli surfaces and differentials on a particular isentropic surface are related by

$$d\sigma \equiv c_p dT + g dz = -d(\mathbf{v} \cdot \mathbf{v}/2). \tag{4.11}$$

This equation is used in the next section to provide a realistic temperature field for the model.

5. Formula for baroclinic vorticity in a horizontally homogeneous environment

Numerical simulations of the first 3–4 h of squall lines and supercell storms generally are based on the assumption of a horizontally homogeneous environment so that they can be initialized from a single sounding (e.g., Weisman 1993; Rotunno and Klemp 1985, respectively). Since a horizontally homogeneous environment is in equilibrium only if the earth's rotation is neglected, we assume that the Rossby number is infinite ($\boldsymbol{\Omega} = 0$). Adopting these assumptions in the present model allows the formula (3.13) for baroclinic vorticity to be cast in a different form. All parcels with the same entropy S now must originate from the same height $h_{-\infty}(S)$ with the same original temperature (where environmental values at upstream infinity are denoted by subscript $-\infty$). Scale analysis of (4.11) indicates that in steady flow, enthalpy differences on a particular isentropic surface Σ are associated almost entirely with differences in potential energy rather than differences in kinetic energy provided that $F^2 \equiv U^2/g|D| \ll 1$, where U^2 and $g|D|$ are measures of changes in kinetic and potential energy, and F is a Froude number. For example, the temperature change owing to a 500-m change in elevation (4.9 K) is much larger than that owing to a 500 $m^2\ s^{-2}$ change in kinetic energy (0.5 K). This is consistent with Betts's (1974) and Darkow's (1986) deductions that the static energy of parcels is nearly conserved. Thus the temperature field can be obtained to a good approximation by imposing constancy of static energy on each isentropic surface. This assumption naturally breaks down in very high-speed flows such as tornadoes but is nevertheless useful in tornadogenesis studies that are concerned with how larger scales of slower motion generate the tornado. Note that the kinetic energy of the irrotational primary flow, $(\nabla\phi)^2/2$, is a known quantity and, if essential in some applications, could be included in a more complicated version of the model.

The new form of (3.13) is derived as follows. Let $h(x, y, h_{-\infty}, t)$ be the height of a particular isentropic or Bernoulli surface Σ with height $h_{-\infty}$ at $x = -\infty$ and let $h'(x, y, h_{-\infty}, t) \equiv h(x, y, h_{-\infty}, t) - h_{-\infty}$ be the height deviation. Since $S(x, y, h(x, y, h_{-\infty}, t), t)$ = constant, $0 = \nabla_S S = \nabla_z S + (\partial S/\partial z)\nabla_S h$, and hence

$$\nabla S = \frac{\partial S}{\partial z}\left[-\left(\frac{\partial h}{\partial x}\right)_S, -\left(\frac{\partial h}{\partial y}\right)_S, 1\right]. \tag{5.1}$$

As justified above, the temperature on Σ is given to a good approximation by

$$T(x, y, h_{-\infty}, t) = T_{-\infty}(h_{-\infty}) - \Gamma_d h'(x, y, h_{-\infty}, t), \tag{5.2}$$

where $\Gamma_d \equiv g/c_p$ is the dry adiabatic lapse rate. The corresponding expression for Λ on Σ is

$$\Lambda(x, y, h_{-\infty}, t) \equiv T_{-\infty}(h_{-\infty})t - \Gamma_d H(x, y, h_{-\infty}, t), \tag{5.3}$$

where

$$H(x, y, h_{-\infty}, t) \equiv \int_0^t h'\, d\hat{t}_P \tag{5.4}$$

is the cumulative height perturbation (henceforth abbreviated to cumulative height) of the parcel currently at (x, y). From (3.13), (5.1), and (5.3), the baroclinic vorticity on Σ is given by

$$\boldsymbol{\omega}_{\mathrm{BC}} \equiv (\xi_{\mathrm{BC}}, \eta_{\mathrm{BC}}, \zeta_{\mathrm{BC}}) = N^2\left[-\left(\frac{\partial H}{\partial y}\right)_S, \left(\frac{\partial H}{\partial x}\right)_S, \left(\frac{\partial H}{\partial x}\right)_S\left(\frac{\partial h}{\partial y}\right)_S - \left(\frac{\partial H}{\partial y}\right)_S\left(\frac{\partial h}{\partial x}\right)_S\right], \tag{5.5}$$

where $N^2 \equiv (g/c_p)\partial S/\partial z$ is the static stability or the square of the *local* Brunt–Väisälä frequency ($N^2 < 0$ for unstable stratification). The scalar product of (5.1) and (5.5) confirms that this solution satisfies the constraint of zero baroclinic potential vorticity $\boldsymbol{\omega}_{\mathrm{BC}} \cdot \boldsymbol{\nabla} S = 0$ deduced in section 3.

The vorticity field described by (5.5) has the following properties. The vortex lines of the horizontal baroclinic vorticity field on Σ are the contours of H with higher (lower) values of accumulated height lying to the right of the vorticity vectors when N^2 is positive (negative). In a horizontal plane, the horizontal vorticity vector has warmer (cooler) cumulative temperature to its left (right). The formula for vertical baroclinic vorticity can be rewritten as

$$\zeta_{\mathrm{BC}} = N^2\mathbf{k} \cdot (\boldsymbol{\nabla}_S H \times \boldsymbol{\nabla}_S h). \tag{5.6}$$

Thus, the vertical vorticity on Σ is proportional to N^2 and the number of solenoids of H and h per unit area. Yet another expression for ζ_{BC} is

$$\zeta_{\mathrm{BC}} = (\xi_{\mathrm{BC}}, \eta_{\mathrm{BC}}) \cdot \boldsymbol{\nabla}_S h, \tag{5.7}$$

a restatement that the potential vorticity is zero and hence the baroclinic vortex lines lie in Σ. The vertical vorticity is cyclonic (anticyclonic) wherever the horizontal vorticity vectors point across the height contours toward higher (lower) values. Scale analysis performed on (5.4) and (5.5) yields $H \sim DL_x/U$ and $(\xi, \eta, \zeta)_{\mathrm{BC}} \sim (N^2D/U)(L_x/L_y, 1, D/L_y)$, where L_x and L_y are characteristic length scales for estimating gradients in the x and y directions, D (which may be positive or negative) is the maximum vertical displacement of Σ, and L_x/U is the appropriate (advective) timescale. Thus, vertical vorticity is small compared to the horizontal vorticity when $|D| \ll \sqrt{L_x^2 + L_y^2}$ or $|\boldsymbol{\nabla}_S h| \ll 1$.

We now demonstrate that the cumulative height H in a zero PV flow serves as a ''streamfunction'' for the vorticity field in both steady and unsteady flow by comparing it to the streamfunction for mass flux along the isentropic surfaces of a *steady* flow. (In an unsteady flow the streamlines are not contained in the isentropic surfaces and this particular streamfunction does not exist.) The continuity equation for steady isentropic flow in $(x, y, h_{-\infty})$ coordinates is

$$\left(\frac{\partial}{\partial x}\right)_S\left(\rho u\frac{\partial h}{\partial h_{-\infty}}\right) + \left(\frac{\partial}{\partial y}\right)_S\left(\rho v\frac{\partial h}{\partial h_{-\infty}}\right) = 0 \tag{5.8}$$

[from straightforward adaptation of Dutton 1976, p. 247, Eq. (50)]. We can define a streamfunction for mass flux ψ (used in later sections) that applies to the flow in a surface of constant $h_{-\infty}$ by

$$\rho v(x, y, h_{-\infty}) = \frac{\partial h_{-\infty}}{\partial z}\left(\frac{\partial \psi}{\partial x}\right)_S,$$

$$\rho u(x, y, h_{-\infty}) = -\frac{\partial h_{-\infty}}{\partial z}\left(\frac{\partial \psi}{\partial y}\right)_S \tag{5.9}$$

because $(\partial h/\partial h_{-\infty})^{-1} = \partial h_{-\infty}/\partial z$. Since the constant-$h_{-\infty}$ surfaces are material surfaces, the vertical velocity of steady flow is given by

$$w(x, y, h_{-\infty}) = \left[\frac{dh(x, y, h_{-\infty})}{dt}\right]_S = \frac{1}{\rho}\frac{\partial h_{-\infty}}{\partial z}\left[\left(\frac{\partial \psi}{\partial x}\right)_S\frac{\partial h}{\partial y} - \left(\frac{\partial \psi}{\partial y}\right)_S\frac{\partial h}{\partial x}\right]. \tag{5.10}$$

Combining (5.9) and (5.10) yields an expression for steady-state velocity,

$$\rho\mathbf{v}(x, y, h_{-\infty}) = \frac{\partial h_{-\infty}}{\partial z}\left[-\left(\frac{\partial \psi}{\partial y}\right)_S, \left(\frac{\partial \psi}{\partial x}\right)_S, \left(\frac{\partial \psi}{\partial x}\right)_S\left(\frac{\partial h}{\partial y}\right)_S - \left(\frac{\partial \psi}{\partial y}\right)_S\left(\frac{\partial h}{\partial x}\right)_S\right]. \tag{5.11}$$

Since the static stability

$$N^2 \equiv \frac{g}{c_p}\frac{\partial S}{\partial z} = \frac{g}{c_p}\frac{\partial S}{\partial h_{-\infty}}\frac{\partial h_{-\infty}}{\partial z} = N_{-\infty}^2\frac{\partial h_{-\infty}}{\partial z}, \tag{5.12}$$

the formula (5.5) for baroclinic vorticity has the same form as (5.11) with $N_{-\infty}^2 H$ taking the place of ψ.

Comparing the solenoid vector in the vorticity equation, $\boldsymbol{\nabla} T \times \boldsymbol{\nabla} S$, to the baroclinic vorticity $\boldsymbol{\omega}_{\mathrm{BC}} \equiv \boldsymbol{\nabla}\Lambda \times \boldsymbol{\nabla} S$ is of some interest. Both these vector fields are solenoidal and so have vector tubes (Borisenko and Tarpov 1979, p. 218). (The vector tubes of $\boldsymbol{\omega}_{\mathrm{BC}}$ are simply the baroclinic vortex tubes.) As found above, the contours of H are the vortex lines of baroclinic vorticity projected onto a horizontal plane. The solenoid vector is given by

$$\boldsymbol{\nabla} T \times \boldsymbol{\nabla} S = \begin{vmatrix} \mathbf{i} & \mathbf{j} & \mathbf{k} \\ \left(\frac{\partial T}{\partial x}\right)_S + \frac{\partial T}{\partial S}\frac{\partial S}{\partial x} & \left(\frac{\partial T}{\partial y}\right)_S + \frac{\partial T}{\partial S}\frac{\partial S}{\partial y} & \frac{\partial T}{\partial S}\frac{\partial S}{\partial z} \\ \frac{\partial S}{\partial x} & \frac{\partial S}{\partial y} & \frac{\partial S}{\partial z} \end{vmatrix} = \begin{vmatrix} \mathbf{i} & \mathbf{j} & \mathbf{k} \\ \left(\frac{\partial T}{\partial x}\right)_S & \left(\frac{\partial T}{\partial y}\right)_S & 0 \\ \frac{\partial S}{\partial x} & \frac{\partial S}{\partial y} & \frac{\partial S}{\partial z} \end{vmatrix}.$$

Inserting $\boldsymbol{\nabla}_S T = -\Gamma_d \boldsymbol{\nabla}_S h$ from (5.2) and $\boldsymbol{\nabla}_z S = -(\partial S/\partial z)\boldsymbol{\nabla}_S h$ from (5.1) yields

$$\nabla T \times \nabla S = N^2\left[-\left(\frac{\partial h}{\partial y}\right)_S, \left(\frac{\partial h}{\partial x}\right)_S, 0\right]. \quad (5.13)$$

Unlike the baroclinic vorticity, the solenoid vector has no vertical component. Its vector lines are the height contours of Σ, and its sense is such that higher (lower) height lies on its right side when N^2 is positive (negative). In a horizontal plane, the solenoid vector has warmer (cooler) temperature to its left (right).

As a check on the baroclinic vorticity formula (5.5), we show that it has the same form as the one derived from linear theory of flow over a hill by Smolarciewicz and Rotunno (1989). Given that $d\ln\alpha/dt$ is negligible for small vertical displacements (see section 6), the vorticity equation (3.7a) linearized about a base state $\mathbf{v} = (U_0, 0, 0)$, $N^2 = N^2_{-\infty}(h_{-\infty})$ is

$$L(\xi', \eta', \zeta')_{\rm BC} = N^2_{-\infty}(-\partial h'/\partial y, \partial h'/\partial x, 0) \quad (5.14)$$

after use of (5.13). Here $L \equiv (\partial/\partial t + U_0\partial/\partial x)$ is the linear material derivative, and primes denote perturbations from the base state. Introducing H' and canceling the L operator (permissible if the perturbations are zero at the start of trajectories) yields the solution

$$(\xi', \eta', \zeta')_{\rm BC} = N^2_{-\infty}(-\partial H'/\partial y, \partial H'/\partial x, 0). \quad (5.15)$$

Second-order baroclinic vertical vorticity $\zeta''_{\rm BC}$ is produced from tilting of first-order horizontal vorticity. Hence

$$L\zeta''_{\rm BC} = N^2_{-\infty}\frac{\partial(H', w')}{\partial(x, y)} = N^2_{-\infty}\frac{\partial(H', Lh')}{\partial(x, y)} = N^2_{-\infty}L\frac{\partial(H', h')}{\partial(x, y)}, \quad (5.16)$$

which has the solution

$$\zeta''_{\rm BC} = N^2_{-\infty}\frac{\partial(H', h')}{\partial(x, y)} = \xi'\frac{\partial h'}{\partial x} + \eta'\frac{\partial h'}{\partial y}. \quad (5.17)$$

Note that $(\xi', \eta', \zeta'')_{\rm BC}$ satisfies the zero potential vorticity requirement and has the same form as the nonlinear baroclinic vorticity (5.5). Smolarciewicz and Rotunno assumed steady hydrostatic flow. For steady flow, $\partial H'/\partial x = h'/U_0$, and (5.15) and (5.17) reduce to their solutions. The expressions for vorticity are the same for hydrostatic and nonhydrostatic flow.

6. The range of validity of the primary–secondary flow approach

All of the above formulas are strictly valid only for dry, inviscid, isentropic flow; and the ones in section 5 depend additionally on the assumptions of high Rossby number, moderate wind speeds, and a horizontally homogeneous environment upstream. In numerically simulated flows that are controlled largely by inviscid, isentropic dynamics, the formulas can be used to diagnose the origins of vortices. Rotunno and Klemp (1985) and Davies-Jones and Brooks (1993) adopted a similar approach in simulations of supercell thunderstorms but used circulation instead of baroclinic vorticity. A simpler approach, based on specifying a simple potential flow as a relevant primary flow and computing the vorticity of the secondary flow, is taken here in order to reveal the origins of vorticity and the fundamental vorticity dynamics. This method has the advantage that the Lagrangian quantities can be computed directly but is limited to applications where the secondary wind is relatively small.

The Boussinesq continuity equation $\nabla\cdot\mathbf{v} = 0$, which omits the compressibility term $d\ln\alpha/dt$, is assumed for the sake of a simple potential flow. From scale analysis of the anelastic continuity equation $\nabla\cdot[\rho_{-\infty}(z)\mathbf{v}] = 0$, it is evident that the Boussinesq version is valid when the vertical displacement of parcels ($\sim D$) is much smaller than the density scale height $H_\rho \equiv -(d\ln\rho_{-\infty}/dz)^{-1}$ (Bannon 1996), where $H_\rho \approx 11$–12 km in the lower few kilometers of an adiabatic atmosphere with a potential temperature of 288 K. Assuming that the appropriate length for scaling $\partial w/\partial z$ is $|D|/2$ (Dutton 1976, p. 491), the Boussinesq approximation applies for $\Xi \equiv |D|/2H_\rho \ll 1$ or $|D| < 3$ km. The equation set thus becomes

$$\partial\mathbf{v}/\partial t - \mathbf{v}\times\boldsymbol{\omega} = -\nabla(c_pT + gz + \mathbf{v}^2/2) + T\nabla S. \quad (6.1)$$

$$\nabla\cdot\mathbf{v} = 0, \quad (6.2)$$

$$\partial S/\partial t + \mathbf{v}\cdot\nabla S = 0, \quad (6.3)$$

$$\boldsymbol{\omega} = \nabla\times\mathbf{v}. \quad (6.4)$$

Assume a steady irrotational, unstratified primary flow (denoted by subscript 1) with uniform velocity $U_0\mathbf{i}$ at upstream infinity ($x = -\infty$) in an isentropic atmosphere of entropy S_0. Then $\mathbf{v}_1 = \nabla\phi_1$, $\nabla^2\phi_1 = 0$, $\boldsymbol{\omega}_1 = 0$, $S_1 = S_0$, where the Bernoulli function $B_1 \equiv c_pT_1 + gz + (\nabla\phi_1)^2/2$ is a universal constant. If $F^2 \ll 1$, $T_1 \approx \theta_0 - \Gamma_d z$, where θ_0 is the potential temperature based on the reference level $z = 0$ instead of 1000 mb.

We now introduce stratification and vertical shear into the environment as secondary effects, and the solutions to second order take the forms $S = S_0 + S_2(h_{-\infty})$, $T = \theta_0 - \Gamma_d h + T_2(h_{-\infty})$, $\mathbf{v} = \mathbf{v}_1 + \mathbf{v}_2$, $\boldsymbol{\omega} = \boldsymbol{\omega}_2 = \boldsymbol{\omega}_{\rm BC} + \boldsymbol{\omega}_{\rm BT}$, $N^2 = N^2_2$, $H = H_1$, $h - h_{-\infty} \equiv h' = h_1$, where the enviromental flow at upstream infinity is $U = U_0 + U_2(h_{-\infty})$, $V = V_2(h_{-\infty})$. From the curl of (6.1) and the definitions of $\boldsymbol{\omega}_{\rm BT}$ and $\boldsymbol{\omega}_{\rm BC}$,

$$\partial\boldsymbol{\omega}_{\rm BT}/\partial t - \nabla\times[(\mathbf{v}_1 + \mathbf{v}_2)\times\boldsymbol{\omega}_{\rm BT}] = 0, \quad (6.5a)$$

$$\partial\boldsymbol{\omega}_{\rm BC}/\partial t - \nabla\times[(\mathbf{v}_1 + \mathbf{v}_2)\times\boldsymbol{\omega}_{\rm BC}] = \nabla T_1\times\nabla S_2, \quad (6.5b)$$

since $\nabla T_2\times\nabla S_2 = 0$. Entropy conservation to second order is given by

$$(\mathbf{v}_1 + \mathbf{v}_2)\cdot\nabla S_2 = 0 \quad (6.6)$$

because S_2 is not a function of time. The assumption

that $S_2 = S_2(h_{-\infty})$, that is, that the isentropic surfaces coincide approximately with the material surfaces of the primary flow that are level at upstream infinity, is valid only if $|\mathbf{v}_2| \ll |\mathbf{v}_1|$. Under this condition the barotropic and baroclinic vorticity then can be computed from (3.10) and (3.13) using the Lagrangian coordinates and the cumulative temperature field of the primary flow. The secondary velocity $\mathbf{v}_2$ then can be recovered from $\nabla \cdot \mathbf{v}_2 = 0$, $\nabla \times \mathbf{v}_2 = \boldsymbol{\omega}_2$, which follow from (6.2) and (6.4), and the boundary conditions. It is convenient to decompose $\mathbf{v}_2$ into rotational parts $\mathbf{v}_{\mathrm{BC}}$ and $\mathbf{v}_{\mathrm{BT}}$ satisfying $\nabla \times \mathbf{v}_{\mathrm{BC}} = \boldsymbol{\omega}_{\mathrm{BC}}$, $\nabla \times \mathbf{v}_{\mathrm{BT}} = \boldsymbol{\omega}_{\mathrm{BT}}$ with the boundary conditions $\mathbf{v}_{\mathrm{BC}} = 0$ and $\mathbf{v}_{\mathrm{BT}} = \mathbf{V}_2$ at upstream infinity, and a potential part $\nabla\phi_2$ subject to $\nabla^2\phi_2 = -\nabla \cdot (\mathbf{v}_{\mathrm{BC}} + \mathbf{v}_{\mathrm{BT}})$, which adjusts $\mathbf{v}_2$ to satisfy other boundary conditions and conservation of volume.

The primary–secondary flow approach is strictly valid when $|\mathbf{v}_2| \ll |\mathbf{v}_1|$. Since the secondary flow arises from baroclinic generation of vorticity and stretching of vortex tubes and $\nabla\phi_2$ is an adjustment, $\mathbf{v}_2$ should have the same magnitude as the larger of $\mathbf{v}_{\mathrm{BC}}$ and $\mathbf{v}_{\mathrm{BT}}$. The secondary velocity associated with the baroclinic vorticity can be estimated as follows. Let $\mathbf{v}_{\mathrm{BC}} \equiv -N^2_{-\infty}H\nabla h_{-\infty}$. Note that $\mathbf{v}_{\mathrm{BC}} = 0$ at upstream infinity and that $\nabla \times \mathbf{v}_{\mathrm{BC}} \equiv -N^2_{-\infty}\nabla H \times \nabla h_{-\infty}$. Since $h_{-\infty}$ is a function of S alone, it follows from (5.1) that $\nabla h_{-\infty} = (\partial h_{-\infty}/\partial z)[-(\partial h/\partial x)_S, -(\partial h/\partial y)_S, 1]$. Using this equation and the relationship between the gradients of H along an isentropic surface and along a horizontal surface, $\nabla_S H = \nabla_z H + (\partial H/\partial z)\nabla_S h$, it can be shown that $\nabla \times \mathbf{v}_{\mathrm{BC}}$ equals the right side of (5.5) and hence is the baroclinic vorticity. By scale analysis $\mathbf{v}_{\mathrm{BC}}/U_0 = (N^2_{-\infty}/U_0)(\partial h_{-\infty}/\partial z)H[(\partial h/\partial x)_S, (\partial h/\partial y)_S, -1] \sim (1/\mathrm{Fr}^2)(1, L_x/L_y, L_x/|D|)$, where $\mathrm{Fr} \equiv |U_0/(N_{-\infty}D)|$ is the *internal* Froude number. For the flows considered in this paper, $L_x \sim L_y \gtrsim |D|$, $|\mathbf{v}_1| \sim U_0$ and the secondary velocity owing to stratification is small compared to the primary flow provided that $(|D|/L_x)\mathrm{Fr}^2 \gg 1$. The primary flows used below do not stretch the barotropic vortex tubes to any great extent; that is, $|\nabla X|$ and $|\nabla Y|$ are order 1. Therefore, the secondary velocity $\mathbf{v}_{\mathrm{BT}}$ associated with the environmental shear $d\mathbf{V}_2/dz$ has a magnitude $|\mathbf{v}_{\mathrm{BT}}| \sim |Dd\mathbf{V}_2/dz|$, and the condition $|\mathbf{v}_{\mathrm{BT}}| \ll |\mathbf{v}_1|$ is satisfied when $M \equiv |d\mathbf{V}_2/dz|/|U_0/D| \ll 1$.

7. The irrotational primary flow

The choice of primary flow is dictated by requirements that it be (i) simple enough to carry out the Lagrangian calculations, (ii) irrotational so that the origins of vorticity can be proven unequivocally, (iii) a solution of the equations in the limit of zero shear and stratification so that it approximates the flow in weakly sheared and stratified environments, and (iv) three-dimensional to allow for the development of secondary vorticity in all directions. Three suitable three-dimensional potential flows are shown in Fig. 1. They are a linear combination of uniform horizontal flow and either a dipole aligned with the flow (case 1), a point source (case 2), or a point source and a point sink farther downstream (case 3) (Batchelor 1967; Lighthill 1986). The first two cases are limits of the third. The dipole is obtained in the limit of zero separation between the source and sink as the strengths of each are increased in inverse proportion to the separation. A point source on its own is obtained by removing the sink to downstream infinity. The uniform flow $U_0\mathbf{i}(U_0 > 0)$ is assumed to be in the positive x direction without loss of generality. All three primary flows are axisymmetric about a horizontal axis, defined as the x axis. The horizontal plane containing the x axis serves as the reference level $z = 0$ for height. Upstream of the source in all three cases, there is a stagnation point at $(x_s, 0, 0)$ that lies on a ''dividing stream tube'' that divides fluid emanating from the source from fluid that has come from upstream infinity (Fig. 1). (In cases 1 and 3 there is also a downstream stagnation point.) W. Rankine recognized during the nineteenth century that utilizing only the part of the flow outside the dividing stream tube yielded steady inviscid irrotational flow around a streamlined solid body of revolution, which is a sphere, a semi-infinite axisymmetric fairing, or a Rankine ovoid in cases 1–3, respectively. A solid surface can be inserted along any stream surface (see Batchelor 1967, p. 453). In fact, inserting a ground surface along one of the upper, outer stream surfaces in case 1 and discarding the flow beneath the ground yields flow over a hill of the shape used by Crapper (1959), Smith (1980), and Smolarkiewicz and Rotunno (1989). The domain of the present model is restricted to regions outside the dividing stream tube that are either totally above or below the $z = 0$ plane in order to to avoid the singularities at the stagnation points (Hawthorne and Martin 1955; Eames and Hunt 1997).

In Part II, the model is applied to air that is chilled by evaporation of rain, becomes negatively buoyant, and descends to near the ground before possibly flowing into a downstream updraft and being forced upward by pressure-gradient forces. The domain for this type of flow is below the $z = 0$ plane. Although the disturbance decays rapidly with distance from the origin, none of the stream surfaces are exactly flat. Modeling a precisely flat ground (at some negative value of z) would require mirror image dipoles and sources and sinks below the ground. This technique was not adopted here because it destroys the axisymmetry of the flow, it makes the problem virtually intractable, and it modifies the solution appreciably only if the ground is close to the dividing stream tube.

Each of the primary flows $\mathbf{v}_1$ has a potential ϕ_1 defined by $\mathbf{v}_1 = \nabla\phi_1$ and, by virtue of the axisymmetry, a Stoke's streamfunction Ψ_1 defined in cylindrical coordinates (x, β, r) with orthonormal basis $\mathbf{i}$, $\hat{\boldsymbol{\beta}}$, $\hat{\mathbf{r}}$ by $u_1(x, r) = (1/\rho_1 r)(\partial\Psi_1/\partial r)$, $v_1(x, r) = -(1/\rho_1 r)(\partial\Psi_1/\partial x)$, where $r \equiv (y^2 + z^2)^{1/2}$, $\beta \equiv \tan^{-1}(z/y)$ and $\mathbf{v}_1(x, r) \equiv (u_1, 0, v_1)$. We assume that $\Xi \ll 1$ so that the Boussinesq continuity equation applies and density can be omitted

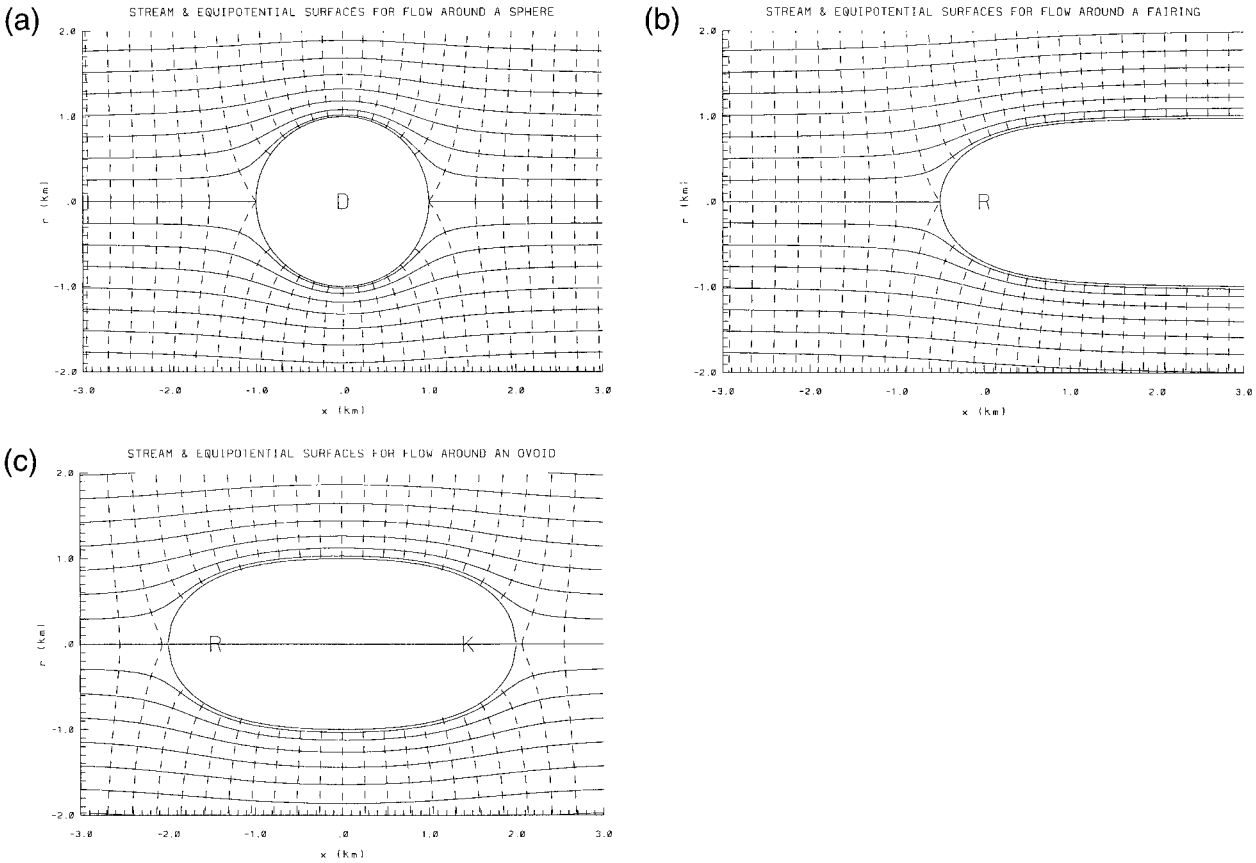

FIG. 1. (a) The stream (solid) and equal potential (dashed) lines in the $y = 0$ plane for three-dimensional irrotational flow around some stationary obstacles of width 2 km: (a) a sphere, (b) a fairing, and (c) a Rankine ovoid. In each case the flow is in the positive x direction and is uniform at upstream infinity. The stream surfaces are the surfaces of revolution obtained by revolving the streamlines about the x axis, and r is distance from the x axis. Here, D, R, and K mark the locations of the dipole, source, and sink that in the uniform stream give rise to the closed or semi-infinite stream tubes that are coincident with the surfaces of the bodies.

from the definition of streamfunction. For a dipole at the origin in a uniform stream,

$$\phi_1(x, r) = U_0 x\left[1 + \frac{A^3}{2R^3}\right], \tag{7.1}$$

$$\Psi_1(x, r) = \frac{U_0 r^2}{2}\left[1 - \frac{A^3}{R^3}\right], \tag{7.2}$$

where A is the radius of the dividing stream tube ($\Psi_1 = 0$), or more simply "the sphere," and $R \equiv (x^2 + r^2)^{1/2}$ is distance from the origin. The dipole's strength $G = 2\pi U_0 A^3$. The equation of the stream surface of cross-sectional radius $r_{-\infty}$ at upstream infinity ($x = -\infty$) and radius r_∞ at downstream infinity ($x = +\infty$) is

$$r^2\left[1 - \frac{A^3}{(x^2 + r^2)^{3/2}}\right] = r_{\pm\infty}^2. \tag{7.3}$$

Clearly, $r_\infty = r_{-\infty}$ in this case.

For a source of strength J at the origin in a uniform stream,

$$\phi_1(x, r) = U_0[x - a^2/4R], \tag{7.4}$$

$$\Psi_1(x, r) = U_0\left[\frac{r^2}{2} - \frac{a^2 x}{4R} - \frac{a^2}{4}\right], \tag{7.5}$$

where $a = (J/\pi U_0)^{1/2}$ is the radius of the dividing stream tube ($\Psi_1 = 0$) or fairing at downstream infinity. The equation for the stream surfaces that lie outside the dividing stream tube is

$$r^2 - \frac{a^2 x}{2(x^2 + r^2)^{1/2}} = r_{\mp\infty}^2 \pm \frac{a^2}{2}. \tag{7.6}$$

Note that $r_\infty^2 - r_{-\infty}^2 = a^2$ in this case.

For a source of strength J at $x = x_P$ and a sink of strength $-J$ at $x = x_Q$ ($>x_P$) in a uniform stream,

$$\phi_1(x, r) = U_0\left[x - \frac{a^2}{4R_P} + \frac{a^2}{4R_Q}\right], \tag{7.7}$$

$$\Psi_1(x, r) = U_0\left[\frac{r^2}{2} - \frac{a^2(x - x_P)}{4R_P} + \frac{a^2(x - x_Q)}{4R_Q}\right], \tag{7.8}$$

where $R_P \equiv [(x - x_P)^2 + r^2]^{1/2}$ is distance from the source, $R_Q \equiv [(x - x_Q)^2 + r^2]^{1/2}$ is distance from the sink, and $a^2 \equiv J/\pi U_0$. The equation of the ovoid is obtained by setting $\Psi_1 = 0$ in (7.8). The source–sink combination becomes a dipole in the limit $x_Q - x_P \to 0$, $J \to \infty$, $(x_Q - x_P)J \to G$ and a lone source in the limit $x_P \to 0$, $x_Q \to \infty$. As the separation distance between the source and the sink decreases from $3a$ to near zero, the ovoid changes shape from almost the shape of two fairings placed back-to-back to nearly spherical, and its maximum radius (in y–z cross sections) changes from $(3)^{1/3}a$ to nearly a. The equation for the outer stream surfaces is

$$r^2 - \frac{a^2(x - x_P)}{2R_P} + \frac{a^2(x - x_Q)}{2R_Q} = r^2_{\pm\infty}. \quad (7.9)$$

Since the primary flow is axisymmetric and $\mathbf{v}_1 \cdot \hat{\boldsymbol{\beta}} \equiv 0$, the individual streamlines within the stream surfaces are determined in each case by the condition $\beta =$ constant.

8. Height of the Bernoulli surfaces

Applying the vorticity formula (5.5) requires a method for computing the height, slope, and spacing of the Bernoulli surfaces. Let $h_{-\infty}$ denote the original height of a parcel in the primary flow (its height at upstream infinity). Since the flow is steady, streamlines are contained in surfaces of constant $h_{-\infty}$. Entropy, introduced into the problem at second order, is a function of $h_{-\infty}$ alone because it is conserved and the environment is horizontally homogeneous. Environmental shear is likewise introduced into the model as a function of $h_{-\infty}$. Since $h_{-\infty} = h_{-\infty}(S)$, $dh_{-\infty}(S)/dt = 0$, and $\boldsymbol{\omega} \cdot \nabla h_{-\infty} = 0$ at $x = -\infty$, $\boldsymbol{\omega} \cdot \nabla h_{-\infty} = 0$ everywhere by (3.22). Thus the surfaces of constant $h_{-\infty}$ contain the primary streamlines and the secondary vortex lines and are the Bernoulli surfaces (and also isentropic surfaces when the secondary flow is stratified) of the secondary flow. We can find the Bernoulli surfaces as the union of all streamlines with the same value of $h_{-\infty}$. Let $h(x, y, h_{-\infty})$ describe the height of the streamlines. Since β is constant along a streamline, the quantity h/r is also constant; that is, $h/r = h_{-\infty}/r_{-\infty}$ along a streamline. Substituting this condition into (7.3), (7.6), and (7.9) yields the following equations for the height of the Bernoulli surfaces:

$$h^2\left[1 - \frac{A^3}{(x^2 + y^2 + h^2)^{3/2}}\right] = h^2_{-\infty} \quad (8.1)$$

$$h^2\left\{1 - \frac{a^2}{2(y^2 + h^2)}\left[\frac{x}{(x^2 + y^2 + h^2)^{1/2}} + 1\right]\right\} = h^2_{-\infty} \quad (8.2)$$

$$h^2\left\{1 - \frac{a^2}{2(y^2 + h^2)}\left[\frac{x - x_P}{[(x - x_P)^2 + y^2 + h^2]^{1/2}} - \frac{x - x_Q}{[(x - x_Q)^2 + y^2 + h^2]^{1/2}}\right]\right\} = h^2_{-\infty} \quad (8.3)$$

in cases 1–3, respectively. The height at any point (x, y) on a given Bernoulli surface $h_{-\infty}$ is found by solving these equations using Newton's method. For case 1, the height contours are clearly circular as deduced by Hawthorne and Martin (1955) because x and y appear in (8.1) only in the combination $x^2 + y^2$. Surfaces for which $|h_{-\infty}| \le A/2$ (case 1) or $|h_{-\infty}| \le a/2$ (cases 2 and 3) are excluded from the domain in order to to avoid errors associated with integration along streamlines that come close to the singularities at the stagnation points.

The slope of the surfaces is found by differentiating (8.1), (8.2), or (8.3) with respect to x and y, which provides two uncoupled linear algebraic equations in $\partial h/\partial x$ and $\partial h/\partial y$. Solving these equations by elementary techniques yields explicit expressions for $\partial h/\partial x$ and $\partial h/\partial y$ in terms of the independent coordinates x, y, $h_{-\infty}$ and the height h of the isentropic surface. The vertical proximity of the surfaces $\partial h_{-\infty}/\partial z$ is obtained by differentiating (8.1), (8.2), or (8.3) with respect to height.

9. The primary cumulative-height field and secondary baroclinic vorticity

The remaining fields needed for the computation of baroclinic vorticity are the static stability N^2; the cumulative height H, defined in (5.4); and its partial derivatives with respect to x and y on an isentropic surface. The static stability is given immediately by (5.12). The cumulative height is obtained as follows. An individual streamline can be labeled by the isentropic surface $h_{-\infty}$ containing it and $y_{-\infty}$, where $(-\infty, y_{-\infty}, h_{-\infty})$ is its location at upstream infinity. The $y_{-\infty}$ label of the streamline passing through the point (x, y, h) on an isentropic surface $h_{-\infty}$ is

$$y_{-\infty} = (h_{-\infty}/h)y \quad (9.1)$$

from the constancy of β along a streamline. For this streamline we can deduce the values of the Stokes's streamfunction Ψ_1 from (7.2), (7.5), or (7.8), and the streamfunction ψ in the isentropic surface from (5.9). In terms of $y_{-\infty}$ and $h_{-\infty}$, $\Psi_1 = U_0(y^2_{-\infty} + h^2_{-\infty})/2$ and $\psi = -U_0 y_{-\infty}$.

Since x increases monotonically from $-\infty$ to $+\infty$ along the streamlines and the flow is steady so that the trajectories are coincident with the streamlines, the time increment following a parcel $dt_P = dx/u_1$ and H can be expressed as

$$H(x, y_{-\infty}, h_{-\infty}) = \int_{-\infty}^{x} \frac{\overline{h}(\hat{x}, y_{-\infty}, h_{-\infty}) - h_{-\infty}}{\overline{u}_1(\hat{x}, y_{-\infty}, h_{-\infty})}\, d\hat{x}, \quad (9.2)$$

where $\overline{h}(x, y_{-\infty}, h_{-\infty})$ and $\overline{u}_1(x, y_{-\infty}, h_{-\infty})$ are the height and the downstream component (in the x direction) of velocity at locations x along the streamline. The overbars signify that they are different mathematical functions from $h(x, y, h_{-\infty})$ and $u_1(x, y, h_{-\infty})$, respectively. For given $(x, y_{-\infty}, h_{-\infty})$, $\overline{h}$ is obtained by replacing h by $\overline{h}$ and y by $y_{-\infty}\overline{h}/h_{-\infty}$ in (8.1), (8.2), or (8.3) and solving the resulting equation by Newton's method. An ex-

pression for $\overline{u}_1(x, y_{-\infty}, h_{-\infty})$ is obtained by making the substitutions $z = \overline{h}$ and $y = y_{-\infty}\overline{h}/h_{-\infty}$ in $u_1 = (\partial\phi_1/\partial x)_{y,z}$.

From (9.1) and (9.2) the derivative of H with respect to y is

$$\left(\frac{\partial H}{\partial y}\right)_{x,S} = \left(\frac{\partial H}{\partial y_{-\infty}}\right)_{x,S}\left(\frac{\partial y_{-\infty}}{\partial y}\right)_{x,S}$$

$$= h_{-\infty}\left(\frac{1}{h} - \frac{y}{h^2}\frac{\partial h}{\partial y}\right)\left(\frac{\partial H}{\partial y_{-\infty}}\right)_{x,S}, \qquad (9.3)$$

where

$$\frac{\partial H}{\partial y_{-\infty}} = \int_{-\infty}^{x} \frac{\partial}{\partial y_{-\infty}}\left[\frac{\overline{h}(\hat{x}, y_{-\infty}, h_{-\infty}) - h_{-\infty}}{\overline{u}_1(\hat{x}, y_{-\infty}, h_{-\infty})}\right] d\hat{x}$$

$$= \int_{-\infty}^{x}\left[\frac{1}{\overline{u}_1}\frac{\partial \overline{h}}{\partial y_{-\infty}} - \frac{\overline{h} - h_{-\infty}}{\overline{u}_1^2}\frac{\partial \overline{u}_1}{\partial y_{-\infty}}\right] d\hat{x}, \qquad (9.4)$$

and the derivative of H with respect to x is

$$\left(\frac{\partial H}{\partial x}\right)_{y,S} = \left(\frac{\partial H}{\partial x}\right)_{y_{-\infty},S} + \left(\frac{\partial H}{\partial y_{-\infty}}\right)_{x,S}\left(\frac{\partial y_{-\infty}}{\partial x}\right)_{y,S}$$

$$= \frac{h - h_{-\infty}}{\overline{u}_1} - \frac{y h_{-\infty}}{h^2}\frac{\partial h}{\partial x}\left(\frac{\partial H}{\partial y_{-\infty}}\right)_{x,S}. \qquad (9.5)$$

The improper integrals in (9.2) and (9.4) are divided into two parts. One part from upstream infinity to x_u, a finite but large negative value of x, was determined by linearizing the integrands, substituting the linear solutions provided in appendix B, and performing the integrations analytically. The remaining part from x_u to x was computed using Gaussian quadrature. With $\partial H/\partial x$, $\partial H/\partial y$, $\partial h/\partial x$, $\partial h/\partial y$, and N^2 determined, the baroclinic vorticity is obtained easily from (5.5).

In case 2, the secondary vorticity at downstream infinity can be expressed in a simple form that does not contain the cumulative height. Let $(\infty, y_\infty, h_\infty)$ denote the location at downstream infinity of the streamline that passes through $(-\infty, y_{-\infty}, h_{-\infty})$. From (7.6) and the constancy of β along each streamline,

$$r_\infty^2 - r_{-\infty}^2 = a^2, \qquad (9.6)$$

$$r_{-\infty}/r_\infty = h_{-\infty}/h_\infty = y_{-\infty}/y_\infty. \qquad (9.7)$$

From (9.6) and (9.7) the downstream height of the streamline, $h_\infty(y_\infty)$, is the solution of the equation

$$h_{-\infty} = h_\infty[1 - a^2/(y_\infty^2 + h_\infty^2)]^{1/2}. \qquad (9.8)$$

From differentiation of (9.8),

$$\left(\frac{\partial h_{-\infty}}{\partial h_\infty}\right)_{y_\infty} = \frac{h_\infty}{h_{-\infty}}\left(1 - \frac{a^2 y_\infty^2}{r_\infty^4}\right), \qquad (9.9)$$

$$\left(\frac{\partial h_\infty}{\partial y_\infty}\right)_{h_{-\infty}} = -\frac{a^2 h_\infty y_\infty}{r_\infty^4 - a^2 y_\infty^2}. \qquad (9.10)$$

The static stabilities far upstream and far downstream are related by

$$N_\infty^2 \equiv \frac{g}{c_p}\frac{\partial S}{\partial h_\infty} = \frac{g}{c_p}\frac{\partial S}{\partial h_{-\infty}}\frac{\partial h_{-\infty}}{\partial h_\infty} = N_{-\infty}^2\frac{\partial h_{-\infty}}{\partial h_\infty}. \qquad (9.11)$$

As $x \to \infty$ $\mathbf{v}_1 \to (U_0, 0, 0)$, $dt \to dx/U_0$ and the gradient of cumulative height in the x-direction

$$\partial H/\partial x \equiv \frac{\partial}{\partial x}\int_0^\infty h'\, d\hat{t}_P \to (h_\infty - h_{-\infty})/U_0. \qquad (9.12)$$

Since the temperature gradient in the y direction tends to a constant and the velocity $\mathbf{v}_1 \to U_0\mathbf{i}$ as $x \to \infty$, the streamwise vorticity $\xi_{BC} \to \infty$ as x. But $\partial h/\partial x \to 0$ as x^{-3} from $\partial/\partial x$ of (8.2) and hence $\xi_{BC}\partial h/\partial x \to 0$ as x^{-2}. Therefore the vertical vorticity at downstream infinity is due entirely to the term $\eta_{BC}\partial h/\partial y$ in (5.7). From (5.5) and (9.9)–(9.12), the baroclinic vorticity far downstream is

$$(\xi_{BC}, \eta_{BC}, \zeta_{BC})_\infty = \frac{N_{-\infty}^2}{U_0}\frac{h_\infty(h_\infty - h_{-\infty})}{h_{-\infty}} \times (\pm\infty, 1 - a^2 y_\infty^2/r_\infty^4, -a^2 h_\infty y_\infty/r_\infty^4), \qquad (9.13)$$

where the + and − signs in ± apply to the left and right sides of the flow, respectively.

The solutions were checked by verifying that

1) results for case 3 tend to those for case 2 as $x_P \to 0$ and $x_Q \to \infty$;
2) results for case 3 tend to those for case 1 in the limit $x_P = -\epsilon$, $x_Q = \epsilon$, $\epsilon \to 0$, $a^2\epsilon \to A^3$;
3) the nonlinear solutions agree with the linear ones in the far field;
4) results for case 2 tend to (9.13) as $x \to \infty$;
5) finite differences of the fields agree with values determined from formulas for the derivatives; and
6) results from the time-dependent linear model derived below in section 11 tend to small-amplitude case 1 results as $t \to \infty$.

10. The direction of baroclinic vorticity

We now deduce the shape of the baroclinic vortex lines, the direction of the vorticity along the vortex lines, and the sign of the vertical vorticity. By a corollary of Helmholtz's theorem, vortex lines cannot begin or end within the fluid, which implies that they must extend to infinity, end on a boundary, or close on themselves (Borisenko and Tarapov 1979, p. 219). We have already found in section 5 that the baroclinic vortex lines lie in isentropic surfaces along contours of the cumulative height H with clockwise (counterclockwise) direction of vorticity along the contours (when viewed from above) when $N^2 D > 0$ (<0). [In horizontal surfaces, warmer (cooler) air is located to the the left (right) of the vorticity vectors.] Note that $H = 0$ at $x = -\infty$ by definition and $H = 0$ at $y = \pm\infty$ where the streamlines

are horizontal and parallel to the x axis. However, $|H|$ is nonzero at downstream infinity ($x = \infty$) in the steady state ($t = \infty$) and increases downstream along each streamline because h' is single-signed in all three cases. Hence, the steady-state baroclinic vortex lines do not close downstream and must be hairpin shaped.

The sign of the baroclinic vertical vorticity is harder to deduce, in general. In terms of seminatural isentropic coordinates ($s, n, h_{-\infty}$), where **s** and **n** are the unit tangent and normal to the horizontal projections of the streamlines (Lilly 1983),

$$\zeta_{\mathrm{BC}} = N^2\left(\frac{\partial H}{\partial s}\frac{\partial h'}{\partial n} - \frac{\partial H}{\partial n}\frac{\partial h'}{\partial s}\right) \tag{10.1}$$

from (5.6). Note that $|\mathbf{v}_1|\partial H/\partial s = h'$ and $|\mathbf{v}_1|\partial h'/\partial s = w_1$. Analogous to (5.7),

$$\zeta_{\mathrm{BC}} = \boldsymbol{\omega}_c\frac{\partial h'}{\partial n} + \boldsymbol{\omega}_s\frac{\partial h'}{\partial s}, \tag{10.2}$$

where $\boldsymbol{\omega}_s \equiv \boldsymbol{\omega}_{\mathrm{BC}} \cdot \mathbf{s}$ and $\boldsymbol{\omega}_c \equiv \boldsymbol{\omega}_{\mathrm{BC}} \cdot \mathbf{n}$ are dubbed here the semistreamwise and semicrosswise baroclinic vorticity (where ''semi'' signifies that they are horizontal components along and normal to the horizontal wind). Thus the vertical baroclinic vorticity may be regarded as the sum of the ''upturns'' of semistreamwise and semicrosswise baroclinic vorticity.

Since $|H|$ increases downstream and $|h'|$ decreases away from the x axis, $\partial H/\partial s$ and $\partial h'/\partial n$ have the same signs as h' and $-h'y$, respectively, for all x in all cases. Thus the upturn of semicrosswise vorticity has the sign of $-N^2y$. Parcels attain their maximum vertical displacements (either positive or negative) at $x = 0$ in cases 1 and 3 and at $x = \infty$ in case 2. At their zenith or nadir points, $\partial h'/\partial s = 0$, the upturn of semistreamwise vorticity is zero, and ζ_{BC} has the sign of $-N^2y$. Downstream of these points (relevant only to cases 1 and 3), $\partial h'/\partial s$ and $\partial H/\partial n$ have the same signs as $-h'$ and $-h'y$, respectively, so that the upturn of semistreamwise vorticity adds to the other upturn and becomes the dominant term in a region in the lee of the hill or depression. Far downstream of the height extremum both terms decay asymptotically to zero. Thus ζ_{BC} has the sign of $-N^2y$ on the leeward side.

Upstream of the zenith or nadir points the upturns tend to cancel one another because $\partial h'/\partial s$ now has the same sign as h' while $\partial H/\partial n$ still has the sign of $-h'y$. Here ζ_{BC} is smaller and its sign is harder to deduce. Consider two parcels A and B in this upstream region that lie at the same current height on the same isentropic surface (Fig. 2). They also have the same original heights $h_{-\infty}$ (at an infinite time ago). In case 1, the height contours are circular and the vertical velocity of the primary flow, $w_1 \equiv \partial\phi_1/\partial z = -3U_0A^3xz/2R^5$, on the height contour decreases in absolute value with increasing $|y|$ (Fig. 2a). In case 2, $w_1 = U_0a^2z/4R^3 \propto 1/R^3$ along the contour, but R, the distance from the origin of points along the contour, increases downstream (Fig. 2b). In case 3, $w_1 = (U_0a^2z/4)(1/R_P^3 - 1/R_Q^3)$ increases in absolute value in the upstream region with decreasing distance from the source and increasing distance from the sink. In all three cases, a parcel on or close to the $y = 0$ plane, A, currently has a larger magnitude of vertical velocity than a parcel farther from this plane, B. Since A is crossing the height contours at a faster rate than B, its trajectory to the current height is nearer the $z = 0$ plane than B's. Thus, in the upstream region $|H|$ increases along the height contour in the direction of increasing $|y|$. For $h' > 0$ (<0), $\nabla h'$ is directed downstream (upstream) and toward (away from) the x axis. In either case, ∇H is left (right) of $\nabla h'$ for $y > 0$ (<0), and ζ_{BC} has the sign of $-N^2y$ in the upstream region. Hence we conclude that (i) the vertical vorticity is purely cyclonic on one side of the flow and purely anticyclonic on the opposite side; and (ii) in the upstream region where the upturns oppose one another, the upturn of semicrosswise baroclinic vorticity is the larger effect. These conclusions are not easily inferred from conventional vorticity analysis based on examining the tilting and stretching terms in the vertical-vorticity equation. Even though there is no lee for stably stratified flow over and past a semi-infinite streamwise ridge (case 2), appreciable cyclonic (anticyclonic) vorticity still forms on the right (left) side of the flow as indicated by the numerous solenoids of H and h in Fig. 2b.

Note that the vertical vorticity is one-signed on a given side of the flow over a hill only near the surface at high Fr where the potential-flow solution is realistic and the vertical-displacement field is nonnegative. If the primary flow were generalized to contain gravity waves, then it is apparent from linear solutions (e.g., Smith 1988, his Fig. 4) that at moderate Fr the cumulative height would be negative for parcels whose upstream heights are a significant fraction of a vertical wavelength. From Smith's (1980) linear solution, Smolarkiewicz and Rotunno (1989, their Fig. 6b) deduced a complicated vortex-line configuration at one-eight of a vertical wavelength aloft. At some Fr < 1 the lowest isentropic surfaces intersect the ground rather than conform to it (Smith 1988, section 14), and the primary flow fails to approximate the actual flow on any isentropic surface.

11. Evolution of the baroclinic vortex lines

The linear time-dependent problem is investigated here to demonstrate that there is a continuous path to the steady-state solution from realistic initial conditions involving gradual evolution of all the fields (velocity, entropy, and vorticity); to show how vertical vorticity develops from a vorticity-free initial state; and to determine the geometric form of the baroclinic vortex lines at early times and at the vortex system's leading edge, which is at downstream infinity in the steady state.

The following derivation for flow over (or under) an obstacle at high Froude number (Fr $\equiv |U_0/ND|$) com-

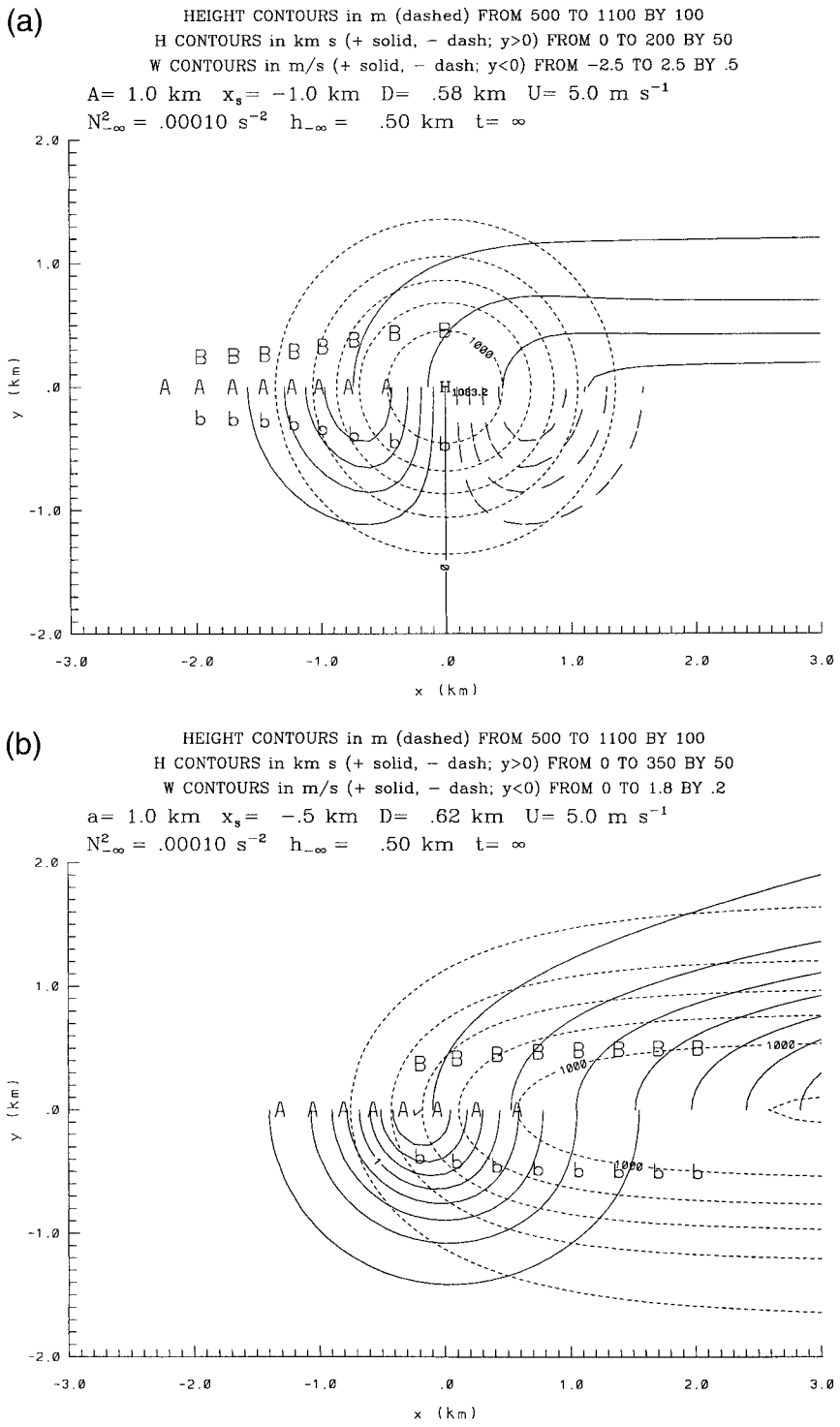

FIG. 2. Backward trajectories for parcels A, B, and b currently on the same isentropic surface at the same current height for (a) flow over an axisymmetric hill (case 1), (b) flow over a semi-infinite streamwise ridge (case 2). Parcel A is in the $y = 0$ plane; B and b are equidistant from this plane on the left and right sides of the flow. The letters mark the locations from right to left of the parcels at the current time: 60 s ago, 120 s ago, . . . , 420 s ago, respectively. The height contours are dashed; the cumulative height contours (shown only for $y > 0$) are solid; and the vertical-velocity contours (shown only for $y < 0$) are solid for positive or zero values, dashed for negative values. The contour and parametric values are indicated on the figures. In each case, the parcel on the axis, A, has a lower trajectory, and hence a lower cumulative height, than the other parcels. Thus the cumulative-height contours cross the height contours toward lower height for increasing $|y|$ as shown.

plements the partly nonlinear analysis of Rotunno and Smolarkiewicz (1991) for flow over and around an obstacle at low Froude number. The flow in Rotunno and Smolarkiewicz's initial-value problem (IVP) is initially at rest (Fr = 0) and is impulsively accelerated irrotationally to a uniform horizontal velocity U_0 so that there is no generation of barotropic or baroclinic vorticity during the start-up process. The isentropic surfaces are level initially and contain a hole if they intersect the obstacle. By deriving initial time tendencies of vorticity and buoyancy out to fourth order, Rotunno and Smolarkiewicz demonstrated that the vorticity develops in the form of initially horizontal, baroclinically generated rings that are tilted to form the lee vortices. They were unable to estimate the intensity of the vortices by this method.

The above IVP is relevant to low Fr flow around solid obstacles or hills but not to flow along initially horizontal isentropic surfaces that are deformed by developing convective updrafts and downdrafts. A high Fr initial-value problem applicable to the latter topic is obtained by considering the gradual inflation of an obstacle in an inviscid uniform flow. The obstacle grows from nothing and approaches its final shape and size, assumed to be a sphere of radius A, asymptotically. The primary flow, which is independent of stratification by definition, remains irrotational. Any material surface of the primary flow that is level at upstream infinity can represent an imperforated isentropic surface that is being uplifted by a penetrative updraft. For the surfaces that lie totally in the far field (i.e., at distances large compared to the obstacle), the vertical displacement is small compared to the width of the perturbation and the problem can be simplified by assuming that the primary flow is uniform. Note that all the isentropic surfaces, except the one coincident with the $z = 0$ plane, lie in the far field initially.

As explained by Lighthill (1986, chapter 8), the flow in the irrotational far field of an expanding object resembles a source flow, and flow past an unchanging solid body is similar at large distances to a dipole in a uniform stream. Thus in our IVP, the outer flow starts out as a source flow and tends toward the dipole flow as time increases. Therefore a permissible choice for the time-varying three-dimensional primary flow is

$$\phi_1(x, y, z, t) = U_0 x + (1 - e^{-\kappa t})\phi_{\text{dipole}}(x, y, z) + e^{-\kappa t}\phi_{\text{source}}(x, y, z), \tag{11.1}$$

where $U_0 x$ is the potential of a uniform stream, $\phi_{\text{dipole}}(x, y, z) = U_0 A^3 x/2R^3$ is the potential of a dipole of strength $G = 2\pi U_0 A^3$, and $\phi_{\text{source}}(x, y, z) = -\kappa A^3/2R$ is the potential of a source of strength $J = 2\pi\kappa A^3$. The nondimensional velocity of the primary flow is

$$\frac{u_1(x, y, z, t)}{U_0} \equiv \frac{1}{U_0}\frac{\partial \phi_1}{\partial x} = 1 + \lambda\frac{x}{R} + \left[\epsilon\left(1 - \frac{3x^2}{R^2}\right) - \lambda\frac{x}{R}\right] \times (1 - e^{-\kappa t}) \tag{11.2a}$$

$$\frac{v_1(x, y, z, t)}{U_0} \equiv \frac{1}{U_0}\frac{\partial \phi_1}{\partial y} = \frac{y}{R}\left[\lambda - \left(3\epsilon\frac{x}{R} + \lambda\right)(1 - e^{-\kappa t})\right] \tag{11.2b}$$

$$\frac{w_1(x, y, z, t)}{U_0} \equiv \frac{1}{U_0}\frac{\partial \phi_1}{\partial z} = \frac{z}{R}\left[\lambda - \left(3\epsilon\frac{x}{R} + \lambda\right)(1 - e^{-\kappa t})\right], \tag{11.2c}$$

where $\epsilon \equiv A^3/2R^3$ and $\lambda \equiv \kappa A^3/2U_0R^2 = \epsilon^{2/3}\kappa A/2^{1/3}U_0$. In the far field, $\epsilon \ll 1$ and $\lambda \ll 1$ as well, provided that the growth timescale κ^{-1} is not too small compared to the advective timescale A/U_0. Under these conditions $u_1 \approx U_0$ and $v_1 \approx 0$, and small vertical displacements ($|h'/h_{-\infty}| = \vartheta(\epsilon) \ll 1$) are governed by the linear equation

$$\frac{\partial h'}{\partial t} + U_0\frac{\partial h'}{\partial x} \equiv w_1(x, y, h_{-\infty}, t) \approx \frac{1}{2}\frac{\kappa e^{-\kappa t}A^3 h_{-\infty}}{(x^2 + y^2 + h_{-\infty}^2)^{3/2}} - \frac{3}{2}U_0(1 - e^{-\kappa t})\frac{A^3 h_{-\infty} x}{(x^2 + y^2 + h_{-\infty}^2)^{5/2}}, \tag{11.3}$$

which has the solution

$$h'(x, y, h_{-\infty}, t) = (1 - e^{-\kappa t})h'_a(x, y, h_{-\infty}), \tag{11.4}$$

where $h'_a(x, y, h_{-\infty}) = (A^3/2)h_{-\infty}(x^2 + y^2 + h_{-\infty}^2)^{-3/2}$ is the steady-state solution. Thus the flow in the far field resembles flow over a hill of the same form first used by Crapper (1959) with a horizontal scale $L = h_{-\infty}$ and a time-dependent (small) height of $D(1 - e^{-\kappa t})$, where $D \equiv A^3/2L^2$. As $t \to \infty$ the solution of the IVP tends to the steady-state solution for flow over a hill of fixed amplitude D. From differentiation of (11.4), the slope of the isentropic surfaces in the far field is

$$\left(\frac{\partial h'}{\partial x}, \frac{\partial h'}{\partial y}\right) = -\frac{3D(1 - e^{-\kappa t})L^3}{(x^2 + y^2 + L^2)^{5/2}}(x, y). \tag{11.5}$$

The assumption of uniform primary flow allows the determination of the components of secondary vorticity by numerical integration because the y coordinate of each parcel is fixed and the x coordinate is a linear function of time. The cumulative height field and its gradients are given by

$$H(x, y, h_{-\infty}, t) \equiv \int_0^t h'(x - U_0 t + U_0\tau, y, h_{-\infty}, \tau)\, d\tau = DL^3 \int_0^t \frac{1 - e^{-\kappa\tau}}{[(x - U_0 t + U_0\tau)^2 + y^2 + L^2]^{3/2}}\, d\tau, \tag{11.6}$$

$$\frac{\partial H}{\partial x}(x, y, h_{-\infty}, t) = \int_0^t \frac{\partial h'}{\partial x}(x - U_0 t + U_0\tau, y, h_{-\infty}, \tau)\, d\tau = -3DL^3 \int_0^t \frac{(1 - e^{-\kappa\tau})(x - U_0 t + U_0\tau)}{[(x - U_0 t + U_0\tau)^2 + y^2 + L^2]^{5/2}}\, d\tau, \tag{11.7}$$

$$\frac{\partial H}{\partial y}(x, y, h_{-\infty}, t) = \int_0^t \frac{\partial h'}{\partial y}(x - U_0 t + U_0\tau, y, h_{-\infty}, \tau)\, d\tau = -3DL^3 y \int_0^t \frac{1 - e^{-\kappa\tau}}{[(x - U_0 t + U_0\tau)^2 + y^2 + L^2]^{5/2}}\, d\tau. \tag{11.8}$$

Inserting the zero-order approximation $N^2 \approx N^2_{-\infty}$ [from (5.12)] and (11.5), (11.7), and (11.8) into (5.5) gives the horizontal components of the secondary vorticity field to first order in ϵ and the second-order vertical component.

The evolution of the vortex lines can be deduced as follows. Under the above assumptions the cumulative height is governed by the linear equation

$$\frac{\partial H}{\partial t} + U_0 \frac{\partial H}{\partial x} = h' = (1 - e^{-\kappa t}) h'_a(x, y, h_{-\infty}). \tag{11.9}$$

This equation can be marched forward in time using a simple forward time difference. Let $H^{(n)} \equiv H(x, y, h_{-\infty}, n\Delta t)$, etc. Since $H(x, y, h_{-\infty}, 0) \equiv 0$ by definition, $H^{(0)} \equiv 0$. From the finite-difference version of (11.9)

$$H^{(n)} = H^{(n-1)} + \Delta t\, h'^{(n-1)} - U_0 \Delta t \frac{\partial H^{(n-1)}}{\partial x}. \tag{11.10}$$

At the first time step $H^{(1)} = 0$. Applying (11.10) recursively yields

$$H^{(n)} = \Delta t \sum_{k=1}^{n-1} h'^{(k)} - U_0 \Delta t \frac{\partial}{\partial x} \sum_{k=2}^{n-1} H^{(k)}. \tag{11.11}$$

Baroclinic generation of vorticity begins at the first time step. At the second time step vortex lines (contours of H) form as horizontal rings collocated with the height contours (as deduced on physical grounds by Scorer 1978, p. 49) and the vector lines of the solenoid vector (section 5). At the third and subsequent time steps, vorticity is still being generated at the local point (x, y) on the isentropic surface, and vorticity produced at previous time steps is being advected downstream. Since potential vorticity is conserved and is zero, the vortex lines remain in the isentropic surface. Therefore displacement and elongation of the H contours in the downstream direction tilts the vortex lines, producing cyclonic (anticyclonic) vertical vorticity on the side of the flow where the vortex lines are directed upslope (downslope). At finite times the H contours and vortex lines are closed because parcels currently at downstream infinity have not been displaced vertically in the time interval $[0, t]$ and thus have zero values of H. On the downstream side of the elongated vortex rings, vorticity increases locally owing to continual baroclinic generation and to positive vorticity advection; at points on the upsteam side, negative vorticity advection offsets some of the generation. In the steady state (at $t = \infty$) the vortex lines open up into hairpin or horseshoe shapes, and at each point negative advection of horizontal vorticity exactly balances baroclinic generation of vorticity.

12. The secondary barotropic vorticity

Effects of weak horizontal vorticity in the environment can be included in the model's secondary flow as follows. A northward component to the environmental wind is included here in order to make the following treatment more general. Assume that the horizontally homogeneous environment is initially undisturbed so that the initial wind is the environmental wind, $\mathbf{V}_0 + \mathbf{V}_2(h_{-\infty}) \equiv (U_0 + U_2, V_0 + V_2, 0)$, and also assume, as in section 6, that $M \equiv |d\mathbf{V}_2/dz|/(|\mathbf{V}_0/D|) \ll 1$ (Drazin 1961). All the parcels in a material surface that is initially level at a height $h_{-\infty}$ have the same value of Z, namely, $h_{-\infty}$. We refer to these material surfaces as constant-Z surfaces. At upstream infinity the flow is assumed to be undisturbed so that far upstream the height of the constant-Z surfaces remains $h_{-\infty}$ and the wind stays the same as the initial wind for all time. In the steady-state limit ($t \to \infty$), the constant-Z surfaces become Bernoulli surfaces because the streamlines lie in the surfaces, and all parcels originate from upstream infinity so that $X \to -\infty$ and $Y \to y_{-\infty}$.

The initial vorticity is $(-dV_2/dZ, dU_2/dZ, 0)$, and so Cauchy's formula (3.10) for the barotropic vorticity becomes

$$\frac{\alpha}{\alpha_0}\begin{bmatrix}\xi_{\rm BT}(x, y, z, t)\\ \eta_{\rm BT}(x, y, z, t)\\ \zeta_{\rm BT}(x, y, z, t)\end{bmatrix} = \begin{bmatrix}\partial x/\partial X & \partial x/\partial Y & \partial x/\partial Z\\ \partial y/\partial X & \partial y/\partial Y & \partial y/\partial Z\\ \partial z/\partial X & \partial z/\partial Y & \partial z/\partial Z\end{bmatrix}\begin{bmatrix}-dV_2/dZ\\ dU_2/dZ\\ 0\end{bmatrix}, \tag{12.1}$$

where α_0 is the original specific volume of a parcel. Equation (12.1) indicates that the barotropic vorticity of a parcel depends on its initial horizontal vorticity and the strain and reorientation of an element of vortex line through its center, and that the parcel acquires vertical barotropic vorticity through tilting of its initially hori-

zontal spin axis. It can be manipulated into a more useful form as follows. Let $\mathbf{J}_{\mathbf{X}}^{\mathbf{x}} \equiv \partial x_i/\partial X_j$ denote the Jacobian matrix in (12.1) of the transformation from Lagrangian to Eulerian coordinates. The equation of continuity in Lagrangian coordinates is $\det(\mathbf{J}_{\mathbf{X}}^{\mathbf{x}}) \equiv \partial(x, y, z)/\partial(X, Y, Z) = \alpha/\alpha_0$ (Dutton 1976, p. 164, 384). The Jacobian matrix of the inverse transformation $\mathbf{J}_{\mathbf{x}}^{\mathbf{X}} \equiv \partial X_i/\partial x_j = (\mathbf{J}_{\mathbf{X}}^{\mathbf{x}})^{-1}$. Hence $\det(\mathbf{J}_{\mathbf{x}}^{\mathbf{X}}) \equiv \partial(X, Y, Z)/\partial(x, y, z) = \alpha_0/\alpha$ and the elements of $\mathbf{J}_{\mathbf{X}}^{\mathbf{x}}$ are related to those of $\mathbf{J}_{\mathbf{x}}^{\mathbf{X}}$ by

$$\frac{\partial x_i}{\partial X_j} = (-1)^{i+j} \times \left(\text{minor of } \frac{\partial X_j}{\partial x_i}\right) \div \det(\mathbf{J}_{\mathbf{x}}^{\mathbf{X}}) = \frac{\alpha}{\alpha_0}(-1)^{i+j} \times \left(\text{minor of } \frac{\partial X_j}{\partial x_i}\right). \tag{12.2}$$

Substituting (12.2) into (12.1) gives

$$\xi_{\mathrm{BT}}(x, y, z, t) = \frac{\partial(Z, X)}{\partial(y, z)}\frac{dU_2}{dZ} + \frac{\partial(Z, Y)}{\partial(y, z)}\frac{dV_2}{dZ} = \frac{\partial(U_2, X)}{\partial(y, z)} + \frac{\partial(V_2, Y)}{\partial(y, z)}, \tag{12.3}$$

$$\eta_{\mathrm{BT}}(x, y, z, t) = \frac{\partial(U_2, X)}{\partial(z, x)} + \frac{\partial(V_2, Y)}{\partial(z, x)}, \tag{12.4}$$

$$\zeta_{\mathrm{BT}}(x, y, z, t) = \frac{\partial(U_2, X)}{\partial(x, y)} + \frac{\partial(V_2, Y)}{\partial(x, y)}. \tag{12.5}$$

Thus,

$$\boldsymbol{\omega}_{\mathrm{BT}} = \boldsymbol{\nabla} \times (U_2\boldsymbol{\nabla}X + V_2\boldsymbol{\nabla}Y) = \boldsymbol{\nabla}U_2 \times \boldsymbol{\nabla}X + \boldsymbol{\nabla}V_2 \times \boldsymbol{\nabla}Y \tag{12.6}$$

Since $\boldsymbol{\nabla}_z X = \boldsymbol{\nabla}_z X + (\partial X/\partial z)\boldsymbol{\nabla}_z z = \boldsymbol{\nabla}_z X + (\partial X/\partial z)[-\boldsymbol{\nabla}_z Z/(\partial Z/\partial z)]$ and $\boldsymbol{\nabla}_z h = -\boldsymbol{\nabla}_z Z/(\partial Z/\partial z)$,

$$\begin{aligned}
\boldsymbol{\nabla}U_2 \times \boldsymbol{\nabla}X &= \frac{dU_2}{dZ}\begin{vmatrix} \mathbf{i} & \mathbf{j} & \mathbf{k} \\ \dfrac{\partial Z}{\partial x} & \dfrac{\partial Z}{\partial y} & \dfrac{\partial Z}{\partial z} \\ \left(\dfrac{\partial X}{\partial x}\right)_Z + \dfrac{\partial X/\partial z}{\partial Z/\partial z}\dfrac{\partial Z}{\partial x} & \left(\dfrac{\partial X}{\partial y}\right)_Z + \dfrac{\partial X/\partial z}{\partial Z/\partial z}\dfrac{\partial Z}{\partial y} & \dfrac{\partial X}{\partial z} \end{vmatrix} \\
&= \frac{dU_2}{dZ}\begin{vmatrix} \mathbf{i} & \mathbf{j} & \mathbf{k} \\ \dfrac{\partial Z}{\partial x} & \dfrac{\partial Z}{\partial y} & \dfrac{\partial Z}{\partial z} \\ \left(\dfrac{\partial X}{\partial x}\right)_Z & \left(\dfrac{\partial X}{\partial y}\right)_Z & 0 \end{vmatrix} \\
&= \frac{dU_2}{dZ}\frac{\partial Z}{\partial z}\begin{vmatrix} \mathbf{i} & \mathbf{j} & \mathbf{k} \\ -\left(\dfrac{\partial h}{\partial x}\right)_Z & -\left(\dfrac{\partial h}{\partial y}\right)_Z & 1 \\ \left(\dfrac{\partial X}{\partial x}\right)_Z & \left(\dfrac{\partial X}{\partial y}\right)_Z & 0 \end{vmatrix}.
\end{aligned} \tag{12.7}$$

Inserting this and a similar expression for $\boldsymbol{\nabla}V_{(2)} \times \boldsymbol{\nabla}Y$ into (12.6) results in

$$\begin{aligned}
\boldsymbol{\omega}_{\mathrm{BT}} = \frac{dU_2}{dh_{-\infty}}\frac{\partial h_{-\infty}}{\partial z} &\times \left[-\left(\frac{\partial X}{\partial y}\right)_Z, \left(\frac{\partial X}{\partial x}\right)_Z, \left(\frac{\partial X}{\partial x}\right)_Z\left(\frac{\partial h}{\partial y}\right)_Z - \left(\frac{\partial X}{\partial y}\right)_Z\left(\frac{\partial h}{\partial x}\right)_Z\right] \\
&+ \frac{dV_2}{dh_{-\infty}}\frac{\partial h_{-\infty}}{\partial z} \\
&\times \left[-\left(\frac{\partial Y}{\partial y}\right)_Z, \left(\frac{\partial Y}{\partial x}\right)_Z, \left(\frac{\partial Y}{\partial x}\right)_Z\left(\frac{\partial h}{\partial y}\right)_Z - \left(\frac{\partial Y}{\partial y}\right)_Z\left(\frac{\partial h}{\partial x}\right)_Z\right].
\end{aligned} \tag{12.8}$$

Note that (12.8) can be decomposed into two parts, each of which has the same form as (5.5). From (12.8) the vertical component of barotropic vorticity in zero-PV flows can be expressed as

$$\zeta_{\mathrm{BT}}(x, y, z, t) = \xi_{\mathrm{BT}}(x, y, z, t)\frac{\partial h}{\partial x} + \eta_{\mathrm{BT}}(x, y, z, t)\frac{\partial h}{\partial y}. \tag{12.9}$$

This equation has been deduced previously by Davies-Jones (1984) and Rotunno and Klemp (1985) and resembles (5.7), the equation for baroclinic vertical vorticity.

Since $X \to -\infty$ as $t \to \infty$, we introduce new coordinates $\overline{x}$ and $\overline{y}$ defined as the position that a parcel would have at the current time t if it had moved in the surface with the environmental wind; that is,

$$\overline{x}(x, y, h_{-\infty}, t) \equiv X + [U_0 + U_2(h_{-\infty})]t,$$
$$\overline{y}(x, y, h_{-\infty}, t) \equiv Y + [V_0 + V_2(h_{-\infty})]t. \tag{12.10}$$

Then (12.8) becomes

$$\begin{aligned}
\boldsymbol{\omega}_{\mathrm{BT}} = \frac{dU_2}{dh_{-\infty}}\frac{\partial h_{-\infty}}{\partial z} &\times \left[-\left(\frac{\partial \overline{x}}{\partial y}\right)_Z, \left(\frac{\partial \overline{x}}{\partial x}\right)_Z, \left(\frac{\partial \overline{x}}{\partial x}\right)_Z\left(\frac{\partial h}{\partial y}\right)_Z - \left(\frac{\partial \overline{x}}{\partial y}\right)_Z\left(\frac{\partial h}{\partial x}\right)_Z\right] \\
&+ \frac{dV_2}{dh_{-\infty}}\frac{\partial h_{-\infty}}{\partial z} \\
&\times \left[-\left(\frac{\partial \overline{y}}{\partial y}\right)_Z, \left(\frac{\partial \overline{y}}{\partial x}\right)_Z, \left(\frac{\partial \overline{y}}{\partial x}\right)_Z\left(\frac{\partial h}{\partial y}\right)_Z - \left(\frac{\partial \overline{y}}{\partial y}\right)_Z\left(\frac{\partial h}{\partial x}\right)_Z\right].
\end{aligned} \tag{12.11}$$

To second order, the barotropic vorticity in a surface of constant Z is the product of the environmental vorticity (second order) and quantities that can be evaluated at first order from the primary flow. In this investigation,

we are interested in the vorticity in an individual Z surface. We assume that the environmental wind in this surface is $U_0\mathbf{i}$ so that the primary flows of section 8 can be used to transport the barotropic vorticity within this surface. At finite times t_1 the variables $\overline{x}$ and $\overline{y}$ are determined by first finding X and Y from trajectories of the primary flow computed backward in time to $t = 0$. Steady-state values of $\overline{x}$ and $\overline{y}$ are obtained by increasing t_1 until the results cease changing discernibly. The streamfunction of the $\boldsymbol{\omega}_{\rm BT}$ field is $(dU_2/dh_{-\infty})\overline{x} + (dV_2/dh_{-\infty})\overline{y}$ by comparison of (12.11) with (5.11).

The barotropic vortex lines are frozen in the flow so their evolution is simple to visualize. For flow over an obstacle that is inflated, loops of vortex lines are drawn upward, resulting in a cyclonic vortex on the right (windward) and an anticyclonic one on the left (leeward) side of the obstacle in the case where the environmental vorticity is purely crosswise (streamwise), as deduced from linear theory by Davies-Jones (1984). The opposite configurations apply to flow under an obstacle. The linear theory assumes that the wind in the basic state is horizontally uniform (i.e., $\overline{x} = x$, $\overline{y} = y$) and thus excludes half the terms in (12.11). It misses the holding back of the barotropic vortex lines in front of the obstacle in the crosswise case as the flow slows to go around the obstacle. This effect, which tilts the loops of vortex lines in the upstream direction and hence results in streamwise (antistreamwise) vorticity on the left (right) lee side of the obstacle, is represented in (12.11) when a three-dimensional potential flow is used as the primary flow (Hawthorne and Martin 1955; Scorer 1978). In the streamwise case, the secondary vortex lines coincide in the steady state with the primary streamlines.

13. The secondary velocity

In the model the primary flow $\mathbf{v}_1(x, y, z, t)$ is prescribed, the constant-Z surfaces are assumed to coincide with those material surfaces of the potential flow that are level at upstream infinity, and secondary vorticity is treated as a passive vector transported by the primary flow, a valid approximation only if the secondary velocity is relatively small. When the secondary vorticity is appreciable, it induces a secondary wind that significantly modifies the parcel trajectories, isentropic surfaces, and static stability. For example, vertical displacements in potential flow decay rapidly with height (or depth) from the source of the disturbance but do not decay in strongly stratified flow (Smith 1979, p. 97). The simple analytical model presented here fails to incorporate these nonlinearities in the primary flow and so misses their effects on the vorticity field. The model does, however, capture some of the qualitative features of the secondary flow and reveal the generation of significant vertical vorticity.

Some of the flow modifications can be deduced from modification of (3.12), which is a *nonunique* decomposition of velocity into an irrotational component and rotational components associated with the baroclinic and barotropic vorticities, for a horizontally homogeneous environment. Inserting (5.3) and the initial wind from section 12 into (3.12) (with $\Omega = 0$) gives

$$\begin{aligned}\mathbf{v} &= -\boldsymbol{\nabla}\Phi - \Gamma_d H\boldsymbol{\nabla}S + T_{-\infty}(S)t\boldsymbol{\nabla}S + (U_0 + U_2)\boldsymbol{\nabla}X \\ &\quad + (V_0 + V_2)\boldsymbol{\nabla}Y \\ &= \boldsymbol{\nabla}(\phi_1 + \chi) - \Gamma_d H\boldsymbol{\nabla}S + U_2\boldsymbol{\nabla}X + V_2\boldsymbol{\nabla}Y, \qquad (13.1)\end{aligned}$$

where $\phi_1 + \chi \equiv -\Phi + t\int T_{-\infty}(S)\,dS + U_0X + V_0Y$. The curl of (13.1) clearly yields the baroclinic vorticity (5.5) [after using (5.1)] plus the barotropic vorticity (12.6). The validity of the velocity field (13.1) can be checked further by determining the circulations associated with it. The baroclinic circulation determined from (13.1) is

$$\begin{aligned}\Gamma_{\rm BC}(t) &= -\Gamma_d \oint_{C(t)} H(x, y, S, t)\boldsymbol{\nabla}S \cdot d\mathbf{x} \\ &= -\Gamma_d \oint_{C(t)} H(x, y, S, t)\,dS, \qquad (13.2)\end{aligned}$$

in agreement with the result of substituting (5.3) into (3.15). The barotropic circulation

$$\Gamma_{\rm BT} = \oint_{C(t)} [U_2(h_{-\infty})\,dX + V_2(h_{-\infty})\,dY] \qquad (13.3)$$

clearly is constant in time and thus satisfies Kelvin's circulation theorem (3.16).

By subtracting the primary velocity $\boldsymbol{\nabla}\phi_1$ from (13.1), introducing the downstream- and lateral-displacement deviations $x' \equiv x - \overline{x}$ and $y' \equiv y - \overline{y}$, and using (12.10), we obtain a nice expression for the secondary velocity,

$$\mathbf{v}_2 = \boldsymbol{\nabla}\phi_2 - \Gamma_d H\boldsymbol{\nabla}S + U_2\mathbf{i} + V_2\mathbf{j} + x'\boldsymbol{\nabla}U_2 + y'\boldsymbol{\nabla}V_2, \qquad (13.4)$$

where $\phi_2 \equiv \chi - U_2x' - V_2y' - (U_2^2 + V_2^2)t/2$. Since S, U_2, and V_2 are functions of $h_{-\infty}$ alone, the secondary velocity can be decomposed (nonuniquely) into an irrotational part $\boldsymbol{\nabla}\phi_2$ and a rotational part $\mathbf{v}_{2\,\rm rot}$ consisting of the imposed environmental shear flow $U_2(h_{-\infty})\mathbf{i} + V_2(h_{-\infty})\mathbf{j}$ and a deviation $\mathbf{v}'_{2\,\rm rot}$ normal to the constant-Z surfaces given by

$$\mathbf{v}'_{2\,\rm rot} = \left(-N^2_{-\infty}H + x'\frac{dU_2}{dh_{-\infty}} + y'\frac{dV_2}{dh_{-\infty}}\right)\boldsymbol{\nabla}h_{-\infty}, \qquad (13.5)$$

which arises from the imbalance in forces normal to the surfaces created by the introduction of shear and/or stratification. The rotational velocity can be split into barotropic and baroclinic parts, as in section 6. It depends on the environmental stability and shear and on primary-flow fields. The adjustment to the velocity field required to satisfy mass continuity and boundary con-

ditions is made through the irrotational component [by a corollary of the derivation in Batchelor (1967), pp. 84–87]. At upstream infinity $H = x' = y' = 0$ so that $\mathbf{v}'_{2\,\mathrm{rot}} = 0$ and hence $\nabla\phi_2 = 0$ there. Thus the potential of the secondary wind is determined by

$$\nabla^2\phi_2 = -\nabla \cdot \mathbf{v}_{2\,\mathrm{rot}}, \tag{13.6}$$

subject to $\nabla\phi_2$ vanishing far upstream and the complete secondary flow being tangential to solid boundaries.

For flows with $N^2H > 0$ such as stably stratified flow over a hill, the rotational velocity associated with the stratification is directed along the downward normal to the isentropic surface because the buoyancy forces are downward. The potential part of the flow must provide for compensating updrafts to satisfy mass continuity, but these updrafts must be located in regions where N^2H has low values in order for (13.2) to hold for arbitrary circuits. The maximum value of $|N^2H|$ is located in the $y = 0$ plane in the lee of the hill or depression. Thus, when $N^2H > 0$ the secondary flow should augment the downdraft in the lee of a hill or reduce the updraft on the downwind side of a depression. This is consistent with the presence of antistreamwise vorticity on the right side of the flow, positive crosswise vorticity on the x axis, and streamwise vorticity on the left side of the flow. The secondary downdraft in the lee is in agreement with Smith's (1980) linear solution that has negative vertical displacements at low levels in the lee of a hill.

The barotropic component of the secondary velocity is the wind induced by the barotropic vortex lines that are present initially (or at upstream infinity for steady flow) and are frozen in the flow. Consider a constant-Z surface where the environmental flow is westerly. Positive speed shear (or crosswise vorticity) in the environment $dU_2/dh_{-\infty} > 0$ is associated with northward vortex lines and stagnation pressure that increases with $h_{-\infty}$. Where the fluid has been delayed by the obstacle, that is, where $x' < 0$, parcels move along the downward normal in response to the downward perturbation pressure-gradient forces that they have encountered. Thus downward motion occurs both on the upstream side and in the wake of an obstacle (Scorer 1978). From a vorticity viewpoint, this downward motion is consistent with increasing vorticity caused by vortex-tube stretching associated with the lagging behind of the central parts of the tubes. Veering of the environmental winds with height, associated with $dV_2/dh_{-\infty} < 0$ and streamwise vortex tubes, induces upward (downward) motion on the right (left) side of the flow where $y' < 0$ (>0). Here the vortex tubes in the $y = 0$ plane are shrinking in decelerating flow, and a vertical-velocity gradient is generated that is consistent with decreasing vorticity. In contrast, Rothfusz and Lilly (1989) and Brooks et al. (1993) found the opposite induced vertical motion—ascent (descent) on the left (right) of the flow—for the case of a sink in a stream with streamwise vorticity because in this case y' is positive (negative) on the right (left) side and the vortex lines are being stretched by the flow as it accelerates toward the sink.

14. Low Froude number effects

The preceding sections explain the origins of vorticity in weakly stratified flow over hills, for example. Since the vorticity is contained in the isentropic surfaces, vertical vorticity is produced as a result of tilting of isentropic surfaces, but there is no vorticity normal to the surfaces because potential vorticity is conserved and remains zero. A recent discovery is the generation of PV in flow over mountains [for a good discussion of this see Schär and Durran (1997)]. The production of PV is by dissipative effects and occurs on a longer timescale than the generation of baroclinic vorticity by the inviscid mechanism modeled in this paper. Since it may be important in the late stages of tornadogenesis, we briefly review the most important findings here.

The Froude number in the initial-value problem posed in section 11 is infinite initially. What happens when the obstacle grows to a height such that the final Froude number is low ($\mathrm{Fr}^2 \ll 1$) and the character of the flow changes from over the obstacle to around it? This evolution is debated by Rotunno and Smolarkiewicz (1991). According to topological fluid dynamics, a hole cannot appear in an isentropic surface in finite time if entropy is conserved (Moffat 1990). It seems intuitive, however, that continual decrease of Fr by inflating an obstacle or decelerating the flow with an applied pressure gradient (Crook et al. 1990) should cause holes to form in some surfaces in finite time. This occurs as a result of turbulent mixing in breaking gravity waves and in regions of isentrope overturning (Crook et al. 1990). Once a hole develops in an isentropic surface, the flow splits to go around instead of over the obstacle, and PV anomalies are generated by slow diffusion in the recirculating wake.

In statistically steady flow, PV anomalies can be generated in isolated regions of dissipation where there is a loss of Bernoulli function along the streamlines (Schär 1993). This is true even if the flow has zero PV initially and zero PV far upstream. Nonconservation of PV following a parcel occurs in the vicinity of surface friction, internal gravity wave breaking, hydraulic jumps, isentrope overturning, isentrope intersections with the ground, internal dissipation, and diabatic heating. For flow over a hill, there is a dissipation region in the lee associated with wave breaking and the wake, and an associated loss of B along the streamlines that pass through this region. The flux of PV, given by $\mathbf{J} = \nabla S \times \nabla B$ from (4.8), was deduced for this flow by Schär (1993, see his Fig. 2). It crosses the region of dissipation from the left to the right side of the flow. Farther downstream the PV fluxes are purely advective (upstream on the left, downstream on the right), resulting in a positive anomaly on the right side and a negative one on the left. At this late stage of vortex formation the lee vortices

are no longer constrained by zero PV to lie along the isentropic surfaces. The sense of the PV anomalies allows the lee vortices to become more vertical. Surface friction then affects the intensity of vortices by inducing radial convergence near the ground and associated vertical stretching. If the vortices are intense enough, surface flow in the lee of the hill becomes reversed owing to the circulations around the cyclonic vortex on the right side of the flow and the anticyclonic one on the left.

15. Conclusions

In this paper, an analytical Lagrangian model for the generation of mesoscale baroclinic vortices at high internal Froude number Fr in inviscid, isentropic flow in horizontally homogeneous nonrotating environments is developed using Dutton's (1976) formulas for baroclinic and barotropic vorticity. The principal results of the theory are as follows. Since potential vorticity is zero initially and is conserved, it remains zero so that the vortex lines lie in the isentropic surfaces, which are material surfaces. The baroclinic vorticity in a particular isentropic surface, zero initially, is determined by the local static stability, N^2, and by horizontal gradients of the height and cumulative heights of parcels in the surface. The barotropic vorticity is found from the property that the barotropic vortex lines are frozen in the flow. The cumulative height, H, of a parcel is defined as the Lagrangian integral of its height perturbation. Horizontal and vertical baroclinic vorticity are given by $(\boldsymbol{\omega}_H)_{\rm BC} = N^2\mathbf{k} \times \boldsymbol{\nabla} H$ and $\zeta_{\rm BC} = N^2\partial(H, h)/\partial(x, y)$, respectively. Thus, the contours of H are the horizontal projections of vortex lines, and $\zeta_{\rm BC}$ is proportional to the local static stability N^2 and the number of solenoids of H and h per unit area. The sense of the horizontal baroclinic vorticity vectors are such that air at the same level has warmer (cooler) cumulative temperature on their left (right) side, and the baroclinic vertical vorticity is positive (negative) where the horizontal vorticity vectors point upslope (downslope). In stably stratified flow through depressions of over axisymmetric hills and growing penetrating tops, vortices form in the lee. It is proven that the vertical baroclinic vorticity is cyclonic (anticyclonic) on the entire right (left) side of the flow, upstream as well as downstream of the height extremum. The opposite configuration of baroclinic vertical vorticity applies for unstably stratified flow. For flow over a hill with positive crosswise vorticity in the environment, the barotropic vortex lines are lifted and partly held back by the obstacle, producing streamwise horizontal and cyclonic vertical vorticity on the right side of the flow, and vorticity of the opposite sense on the left side. For flow through a depression the vertical-vorticity configuration is opposite. For steady flow in environments with purely streamwise vorticity, the barotropic vortex lines coincide with the streamlines; so the barotropic vertical vorticity is cyclonic (anticyclonic) in regions of upward (downward) motion.

Actual fields will be presented in a subsequent article, in which the validity of the model at high Fr will be established by showing that it correctly predicts the secondary streamwise vorticity in the lee of an obstacle (Hawthorne and Martin 1955) and baroclinically generated vortices in the lee of a hill (Smolarkiewicz and Rotunno 1989). The model then will be generalized to apply approximately to flow through saturated downdrafts in conditionally unstable environments and thence to the development of vertical vorticity near the ground in mesocyclones and bow-echo storms.

Acknowledgments. I am indebted to the two anonymous reviewers for providing insightful and thorough reviews, for spotting several errors in the original manuscript, and for suggesting needed clarifications.

APPENDIX A

Proof of Vorticity-Decomposition Theorem

For inviscid, dry, isentropic flow, Dutton (1976) and Mobbs (1981) showed that vector vorticity $\boldsymbol{\omega}(x, y, z, t)$ decomposes into barotropic and baroclinic components. Cauchy's formula (3.10) for barotropic vorticity can be verified as follows (Dutton 1976, p. 385). Substitution of (3.10) into the left side of (3.7a) and using the chain rule yields

$$\frac{1}{\alpha}\frac{d(\alpha\omega_i)}{dt} = \frac{1}{\alpha}(\alpha\omega_k)_{t=0}\left(\frac{\partial}{\partial t}\right)_X\left(\frac{\partial x_i}{\partial X_k}\right) = \frac{1}{\alpha}(\alpha\omega_k)_{t=0}\frac{\partial v_i}{\partial X_k}$$

$$= \frac{1}{\alpha}(\alpha\omega_k)_{t=0}\frac{\partial x_j}{\partial X_k}\frac{\partial v_i}{\partial x_j} = \omega_j\frac{\partial v_i}{\partial x_j}. \qquad \text{(A.1)}$$

Thus, (3.10) satisfies the barotropic version of (3.7) with the initial condition $\boldsymbol{\omega}_{\rm BT}(x, y, z, 0) \equiv \boldsymbol{\omega}(x, y, z, 0)$.

We still need to prove that the formula for baroclinic vorticity in isentropic flow,

$$\boldsymbol{\omega}_{\rm BC}(x, y, z, t) = \boldsymbol{\nabla}\Lambda \times \boldsymbol{\nabla} S, \qquad \text{(A.2)}$$

where $\Lambda \equiv \int_0^t T\, d\tau$ following a parcel, is a solution of the vector vorticity equation (3.7) with initial condition $\boldsymbol{\omega}(x, y, z, 0) \equiv 0$. Dutton provides a direct proof that involves advanced fluid mechanics. A less revealing but easier proof is given here. It consists of a simple check that (A.2) is indeed a solution of the initial-value problem. Clearly, $\boldsymbol{\omega}_{\rm BC}(x, y, z, 0) \equiv 0$. Inserting (A.2) into the left side of (3.7b) yields

$$\frac{\partial\boldsymbol{\omega}_{\rm BC}}{\partial t} + \boldsymbol{\nabla} \times (\boldsymbol{\omega}_{\rm BC} \times \mathbf{v})$$

$$\equiv \frac{\partial(\boldsymbol{\nabla}\Lambda \times \boldsymbol{\nabla} S)}{\partial t} + \boldsymbol{\nabla} \times ([(\boldsymbol{\nabla}\Lambda \times \boldsymbol{\nabla} S) \times \mathbf{v}]). \qquad \text{(A.3)}$$

By vector identities,

$$(\boldsymbol{\nabla}\Lambda \times \boldsymbol{\nabla}S) \times \mathbf{v} \equiv (\mathbf{v}\cdot\boldsymbol{\nabla}\Lambda)\boldsymbol{\nabla}S - (\mathbf{v}\cdot\boldsymbol{\nabla}S)\boldsymbol{\nabla}\Lambda \quad \text{and} \tag{A.4}$$

$$\boldsymbol{\nabla}\times[(\boldsymbol{\nabla}\Lambda\times\boldsymbol{\nabla}S)\times\mathbf{v}] \equiv \boldsymbol{\nabla}(\mathbf{v}\cdot\boldsymbol{\nabla}\Lambda)\times\boldsymbol{\nabla}S - \boldsymbol{\nabla}(\mathbf{v}\cdot\boldsymbol{\nabla}S)\times\boldsymbol{\nabla}\Lambda. \tag{A.5}$$

Therefore, from (A.3) and (A.5),

$$\frac{\partial\boldsymbol{\omega}_{\mathrm{BC}}}{\partial t} + \boldsymbol{\nabla}\times(\boldsymbol{\omega}_{\mathrm{BC}}\times\mathbf{v}) \equiv \boldsymbol{\nabla}\frac{d\Lambda}{dt}\times\boldsymbol{\nabla}S + \boldsymbol{\nabla}\Lambda\times\boldsymbol{\nabla}\frac{dS}{dt} \equiv \boldsymbol{\nabla}T\times\boldsymbol{\nabla}S \tag{A.6}$$

since $dS/dt \equiv 0$. Thus, (3.7b) is satisfied.

Since the vector vorticity equation and the initial conditions are explicitly linear in $\boldsymbol{\omega}$, $\boldsymbol{\omega} = \boldsymbol{\omega}_{\mathrm{BT}} + \boldsymbol{\omega}_{\mathrm{BC}}$ is a general solution of the vector vorticity equation for inviscid, dry, isentropic flows.

The formula (3.12) for absolute velocity can be verified similarly. The material derivatives of the individual terms on the right side of (3.12) in an absolute Cartesian coordinate system are

$$\frac{d}{dt}(\Lambda\boldsymbol{\nabla}S) = T\boldsymbol{\nabla}S + \Lambda\left(\boldsymbol{\nabla}\frac{dS}{dt} - \frac{\partial u_j}{\partial x_i}\frac{\partial S}{\partial x_j}\right) = T\boldsymbol{\nabla}S - \Lambda\frac{\partial u_j}{\partial x_i}\frac{\partial S}{\partial x_j}, \tag{A.7}$$

$$-\frac{d}{dt}\boldsymbol{\nabla}\Phi = -\boldsymbol{\nabla}\frac{d\Phi}{dt} + \frac{\partial u_j}{\partial x_i}\frac{\partial\Phi}{\partial x_j} = -\boldsymbol{\nabla}(c_pT + g_az) + \boldsymbol{\nabla}\frac{\mathbf{u}\cdot\mathbf{u}}{2} + \frac{\partial u_j}{\partial x_i}\frac{\partial\Phi}{\partial x_j}, \tag{A.8}$$

$$\frac{d}{dt}\left[\frac{\partial X_k}{\partial x_i}(u_0)_k\right] = \left[\frac{\partial}{\partial x_i}\frac{dX_k}{dt} - \frac{\partial u_j}{\partial x_i}\frac{\partial X_k}{\partial x_j}\right](u_0)_k = -\frac{\partial u_j}{\partial x_i}\frac{\partial X_k}{\partial x_j}(u_0)_k, \tag{A.9}$$

where we have used (3.5) in (A.7), the definition of Φ in (A.8), and conservation of $\mathbf{X}$ in (A.9). Therefore, the material derivative of (3.12) is

$$\frac{d_a\mathbf{u}}{dt} = T\boldsymbol{\nabla}S - \boldsymbol{\nabla}(c_pT + g_az) + \boldsymbol{\nabla}\frac{\mathbf{u}\cdot\mathbf{u}}{2} - \frac{\partial u_j}{\partial x_i}\left[\Lambda\frac{\partial S}{\partial x_j} - \frac{\partial\Phi}{\partial x_j} + \left(\frac{\partial X_k}{\partial x_j}\right)(u_0)_k\right]$$
$$= T\boldsymbol{\nabla}S - \boldsymbol{\nabla}(c_pT + g_az) + \boldsymbol{\nabla}\frac{\mathbf{u}\cdot\mathbf{u}}{2} - u_j\frac{\partial u_j}{\partial x_i}$$
$$= T\boldsymbol{\nabla}S - \boldsymbol{\nabla}(c_pT + g_az) \tag{A.10}$$

since the expression inside the bracket equals $\mathbf{u}$ from (3.12). Hence (3.12) satisfies (3.3a) for isentropic flow.

APPENDIX B

Linear Solutions for Baroclinic Vorticity

Linear solutions are required for computing the far-field part of the improper integrals in (9.2) and (9.4) and for checking that the nonlinear solutions are correct in the far field. For case 1 (the dipole in a uniform stream), we introduce a parameter that is small in the far field, namely $\epsilon \equiv A^3/2R_0^3$, where $R_0 \equiv (x^2 + y^2 + h_{-\infty}^2)^{1/2}$, and expand h in a power series in ϵ, that is,

$$h(x, y, h_{-\infty}) = h_{-\infty} + \epsilon h_{(1)} + \epsilon^2 h_{(2)} + \cdots. \tag{B.1}$$

The first-order solution of (8.1) is

$$h'(x, y, h_{-\infty}) = \epsilon h_{(1)}(x, y, h_{-\infty}) = \frac{A^3 h_{-\infty}}{2R_0^3}, \tag{B.2}$$

which has the same shape as the hill used by Crapper (1959) and others. The horizontal derivatives of h are

$$\left(\frac{\partial h}{\partial x}, \frac{\partial h}{\partial y}\right) = -\frac{3}{2}\frac{A^3 h_{-\infty}}{R_0^5}(x, y) \tag{B.3}$$

to first order. The cumulative height is defined by

$$H(x, y, h_{-\infty}) = \int_{-\infty}^{x} \frac{\overline{h}(\hat{x}, y_{-\infty}, h_{-\infty}) - h_{-\infty}}{\overline{u}_1(\hat{x}, y_{-\infty}, h_{-\infty})}\, d\hat{x}. \tag{B.4}$$

To first order

$$y_{-\infty} = y\left(1 - \frac{\epsilon h_{(1)}}{h_{-\infty}}\right), \tag{B.5}$$

from (9.1) and

$$u_1(x, y, h_{-\infty}) = U_0\left[1 + \frac{A^3}{2R_0^3} - \frac{3}{2}\frac{A^3x^2}{R_0^5}\right] + \cdots, \tag{B.6}$$

from $\partial/\partial x$ of (7.1). Only the zero-order terms in (B.5) and (B.6) contribute to the linear solution for H; hence

$$H(x, y, h_{-\infty}) = \frac{1}{U_0}\int_{-\infty}^{x} \epsilon h_{(1)}(x, y, h_{-\infty})\, d\hat{x} = \frac{A^3}{2U_0}\frac{h_{-\infty}}{y^2 + h_{-\infty}^2}\left(1 + \frac{x}{R_0}\right). \tag{B.7}$$

The horizontal baroclinic vorticity is

$$\xi_{\mathrm{BC}}(x, y, h_{-\infty}) = \frac{N_{-\infty}^2 A^3}{2U_0}\frac{h_{-\infty}y}{R_0^3}\frac{2R_0 - x}{(R_0 - x)^2}, \tag{B.8}$$

$$\eta_{\mathrm{BC}}(x, y, h_{-\infty}) = \frac{N_{-\infty}^2 A^3}{2U_0}\frac{h_{-\infty}}{R_0^3}, \tag{B.9}$$

to first order from (5.15); and from (5.17) the second-order vertical baroclinic vorticity is

$$\zeta_{\mathrm{BC}}(x, y, h_{-\infty}) = -\frac{3N_{-\infty}^2 A^6}{4U_0}\frac{h_{-\infty}^2 y}{R_0^6(R_0 - x)^2}. \tag{B.10}$$

The linear solutions for case 2 (source in uniform flow) are

$$h'(x, y, h_{-\infty}) = \frac{a^2 h_{-\infty}}{4R_0(R_0 - x)}, \tag{B.11}$$

$$H(x, y, h_{-\infty}) = \frac{a^2}{4U_0}\frac{h_{-\infty}}{(R_0 - x)}, \tag{B.12}$$

$$\xi_{\rm BC}(x, y, h_{-\infty}) = \frac{N_{-\infty}^2 a^2}{4U_0}\frac{h_{-\infty} y}{R_0(R_0 - x)}, \tag{B.13}$$

$$\eta_{\rm BC}(x, y, h_{-\infty}) = \frac{N_{-\infty}^2 a^2}{4U_0}\frac{h_{-\infty}}{R_0(R_0 - x)}, \tag{B.14}$$

$$\zeta_{\rm BC}(x, y, h_{-\infty}) = -\frac{N_{-\infty}^2 a^4}{16U_0}\frac{h_{-\infty}^2 y}{R_0^3(R_0 - x)^3} \tag{B.15}$$

and for case 3 (source and sink in uniform flow) are

$$h'(x,y,h_{-\infty}) = \frac{a^2 h_{-\infty}}{4r_0^2}\left(\frac{x - x_P}{R_{P0}} - \frac{x - x_Q}{R_{Q0}}\right), \tag{B.16}$$

$$\frac{\partial h}{\partial x} = \frac{a^2 h_{-\infty}}{4}\left(\frac{1}{R_{P0}^3} - \frac{1}{R_{Q0}^3}\right), \tag{B.17}$$

$$\frac{\partial h}{\partial y} = -\frac{a^2}{4}\frac{h_{-\infty} y}{r_0^4}\left[2\left(\frac{x - x_P}{R_{P0}} - \frac{x - x_Q}{R_{Q0}}\right) + r_0^2\left(\frac{x - x_P}{R_{P0}^3} - \frac{x - x_Q}{R_{Q0}^3}\right)\right], \tag{B.18}$$

$$H(x,y,h_{-\infty}) = \frac{a^2}{4U_0}\frac{h_{-\infty}}{r_0^2}(R_{P0} - R_{Q0} + x_Q - x_P), \tag{B.19}$$

$$\frac{\partial H}{\partial x} = \frac{a^2}{4U_0}\frac{h_{-\infty}}{r_0^2}\left(\frac{x - x_P}{R_{P0}} - \frac{x - x_Q}{R_{Q0}}\right), \tag{B.20}$$

$$\frac{\partial H}{\partial y} = \frac{a^2}{4U_0}\frac{h_{-\infty} y}{r_0^4} \times \left[r_0^2\left(\frac{1}{R_{P0}} - \frac{1}{R_{Q0}}\right) - 2(R_{P0} - R_{Q0} + x_Q - x_P)\right], \tag{B.21}$$

$$\boldsymbol{\omega}_{\rm BC} \equiv (\xi_{\rm BC}, \eta_{\rm BC}, \zeta_{\rm BC}) = N_{-\infty}^2\left(-\frac{\partial H}{\partial y}, \frac{\partial H}{\partial x}, \frac{\partial H}{\partial x}\frac{\partial h}{\partial y} - \frac{\partial H}{\partial y}\frac{\partial h}{\partial x}\right) \tag{B.22}$$

where $r_0^2 \equiv y^2 + h_{-\infty}^2$, $R_{P0} \equiv [(x - x_P)^2 + r_0^2]^{1/2}$ and $R_{Q0} \equiv [(x - x_Q)^2 + r_0^2]^{1/2}$. From (8.2) and (8.3) the linear solutions are valid in case 2 where $(a^2/2r^2)(1 + x/R) \ll 1$ and in case 3 where $(a^2/2r^2)[(x - x_P)/R_P - (x - x_Q)/R_Q] \ll 1$.

REFERENCES

Bannon, P. R., 1996: On the anelastic approximation for a compressible atmosphere. *J. Atmos. Sci.,* **53,** 3618–3628.

Batchelor, G. K., 1967: *An Introduction to Fluid Mechanics.* Cambridge University Press, 615 pp.

Betts, A. K., 1974: Further comments on ''A comparison of the equivalent potential energy and static energy.'' *J. Atmos. Sci.,* **31,** 1713–1715.

Borisenkov, A. I., and I. E. Tarapov, 1979: *Vector and Tensor Analysis with Applications.* Dover, 257 pp.

Brandes, E. A., 1990: Evolution and structure of the 6–7 May 1985 mesoscale convective system and associated vortex. *Mon. Wea. Rev.,* **118,** 109–127.

Brooks, H. E., C. A. Doswell III, and R. Davies-Jones, 1993: Environmental helicity and the maintenance and evolution of low-level mesocyclones. *The Tornado: Its Structure, Dynamics, Prediction, and Hazards, Geophys. Monogr.,* No. 79, Amer. Geophys. Union, 97–104.

Crapper, G. D., 1959: A three-dimensional solution for waves in the lee of mountains. *J. Fluid Mech.,* **6,** 51–76.

Crook, N. A., T. L. Clark, and M. W. Moncrieff, 1990: The Denver cyclone. Part I: Generation in low Froude number flow. *J. Atmos. Sci.,* **47,** 2725–2742.

Darkow, G. L., 1986: Basic thunderstorm energetics and thermodynamics. *Thunderstorm Morphology and Dynamics,* E. Kessler, Ed., University of Oklahoma Press, 59–73.

Davies-Jones, R. P., 1984: Streamwise vorticity: The origin of updraft rotation in supercell storms. *J. Atmos. Sci.,* **41,** 2991–3006.

——, 1991: The frontogenetical forcing of secondary circulations. Part I: The duality and generalization of the Q vector. *J. Atmos. Sci.,* **48,** 497–509.

——, 1996: Formulas for the baroclinic and barotropic components of vorticity with application to vortex formation near the ground. Preprints, *Seventh Conf. on Mesoscale Processes,* Reading, United Kingdom, Amer. Meteor. Soc., 14–16.

——, and H. E. Brooks, 1993: Mesocyclogenesis from a theoretical perspective. *The Tornado: Its Structure, Dynamics, Prediction, and Hazards, Geophys. Monogr.,* No. 79, Amer. Geophys. Union, 105–114.

Drazin, P. G., 1961: On the steady flow of a fluid of variable density past an obstacle. *Tellus,* **13,** 239–251.

Dutton, J. A., 1976: *The Ceaseless Wind.* McGraw-Hill, 579 pp.

Eames, I., and J. C. R. Hunt, 1997: Inviscid flow around bodies moving in weak density gradients without buoyancy gradients. *J. Fluid Mech.,* **353,** 331–355.

Eckart, C., 1960: Variation principles of hydrodynamics. *Phys. Fluids,* **3,** 421–427.

Haltiner, G. J., and F. L. Martin, 1957: *Dynamical and Physical Meteorology.* McGraw-Hill, 470 pp.

Hawthorne, W. R., and M. E. Martin, 1955: The effect of density gradient and shear on the flow over a hemisphere. *Proc. Roy. Soc. A.,* **232,** 184–195.

Haynes, P. H., and M. E. McIntyre, 1987: On the evolution of vorticity and potential vorticity in the presence of diabatic heating and frictional or other forces. *J. Atmos. Sci.,* **44,** 828–841.

Hildebrand, F. B., 1962: *Advanced Calculus for Applications.* Prentice-Hall, 646 pp.

Kanehisa, H., 1996: A relationship between the Bernoulli function and potential vorticity. *J. Meteor. Soc. Japan,* **74,** 383–386.

Klemp, J. B., and R. Rotunno, 1983: A study of the tornadic region within a supercell thunderstorm. *J. Atmos. Sci.,* **40,** 359–377.

Lighthill, J., 1986: *An Informal Introduction to Fluid Mechanics.* Oxford University Press, 260 pp.

Lilly, D. K., 1983: Dynamics of rotating storms. *Mesoscale Meteorology—Theories, Observations and Models,* D. K. Lilly and T. Gal-Chen, Eds., Reidel, 531–544.

Mobbs, S. D., 1981: Some vorticity theorems and conservation laws for non-barotropic fluids. *J. Fluid Mech.,* **108,** 475–483.

Moffatt, H. K., 1990: The topological (as opposed to analytical) ap-

proach to fluid and plasma physics problems. *Topological Fluid Mechanics, Proceedings of the IUTAM Symposium*, H. K. Moffatt and A. Tsinober, Eds., Cambridge University Press, 1–10.

Rothfusz, L. P., and D. K. Lilly, 1989: Quantitative and theoretical analysis of an experimental helical vortex. *J. Atmos. Sci.,* **46,** 2265–2279.

Rotunno, R., and J. B. Klemp, 1985: On the rotation and propagation of simulated supercell thunderstorms. *J. Atmos. Sci.,* **42,** 271–292.

——, and P. K. Smolarkiewicz, 1991: Further results on lee vortices in low-Froude-number flow. *J. Atmos. Sci.,* **48,** 2204–2211.

Salmon, R., 1988: Hamiltonian fluid mechanics. *Annu. Rev. Fluid Mech.,* **20,** 225–256.

Schär, C., 1993: A generalization of Bernoulli's theorem. *J. Atmos. Sci.,* **50,** 1437–1443.

——, and D. R. Durran, 1997: Vortex formation and vortex shedding in continuously stratified flows past isolated topography. *J. Atmos. Sci.,* **54,** 534–554.

Scorer, R. S., 1978: *Environmental Aerodynamics.* Ellis Horwood, 488 pp.

Serrin, J., 1959: Mathematical principles of classical fluid mechanics. *Handbuch der Physik,* S. Flügge, Ed., Vol. VIII, Springer-Verlag, 125–163.

Smith, R. B., 1979: The influence of mountains on the atmosphere. *Advances in Geophysics,* Vol. 21, Academic Press, 87–230.

——, 1980: Linear theory of stratified hydrostatic flow past an isolated mountain. *Tellus,* **32,** 348–364.

——, 1988: Linear theory of stratified flow past an isolated mountain in isosteric coordinates. *J. Atmos. Sci.,* **45,** 3889–3896.

Smolarkiewicz, P. K., and R. Rotunno, 1989: Low Froude number flow past three-dimensional obstacles. Part I: Baroclinically generated lee vortices. *J. Atmos. Sci.,* **46,** 1154–1164.

Taylor, E. S., 1972: Secondary flow. *Illustrated Experiments in Fluid Mechanics: The National Committee for Fluid Mechanics Films Book of Film Notes,* The MIT Press, 97–104.

Weisman, M. L., 1993: The genesis of severe, long-lived bow echoes. *J. Atmos. Sci.,* **50,** 645–670.

——, and C. A. Davis, 1998: Mechanism for the generation of mesoscale vortices within quasi-linear convective systems. *J. Atmos. Sci.,* **55,** 2603–2622.